

**PREDICTION OF THE HIP JOINT CENTRE FROM
EXTERNALLY PLACED MARKERS IN GAIT
ANALYSIS STUDIES**

By Craig Simpson (BSc)

This thesis is submitted in partial fulfilment of the requirements for the degree of
MSc in Bioengineering

16th August 2011
Bioengineering Unit
University of Strathclyde
Glasgow, UK

This thesis is the result of the author's original research. It has been composed by the author and has not been previously submitted for examination which has led to the award of a degree.

The copyright of this thesis belongs to the author under the terms of the United Kingdom Copyright Acts as qualified by University of Strathclyde Regulation 3.50. Due acknowledgement must always be made of the use of any material contained in, or derived from, this thesis.

Signed:

Date:

ACKNOWLEDGEMENTS

I would like to thank my project supervisor Mr Stephanos Solomonidis for all the help and guidance he provided throughout the duration of this project, showing great patience along the way, which was definitely much appreciated. He always made himself available when I needed help or advice and his contagious enthusiasm and motivation kept me going when stress levels soared. Also I would like to thank the rest of the departmental staff for helping throughout the year and PSAS for providing scholarship funding for my tuition.

I would also like to thank the Math Department, especially my co-supervisor Prof. Oleg Davydov whose assistance was extremely beneficial to my understanding of MATLAB and who provided much needed help and support in development of the code. He has shown great enthusiasm throughout the duration of this project.

Thanks to the staff at the Southern General Hospital who allowed us to use their MRI facilities along with providing useful advice and insight into their department.

I would like to thank my family for the support they have given and to my classmates for keeping spirits high throughout the course, couldn't have done it without you.

ABSTRACT

It is required for gait analysis studies to identify the location of the Hip Joint Centre (HJC). Unlike other joints, the hip joint is located deep within the body; therefore it is extremely difficult to obtain its exact position. In order to determine various joint kinetics such as muscle forces and moments around the hip, it is important that this location is as accurate as possible. Failure to do so can result in major errors in these parameters of up to 20%.

There have been many suggestions put forward in an attempt to accurately determine this location. These take the form of 'predictive' and 'functional' methods. Predictive methods use regression equations based on pelvic geometry and leg length and are preferred in clinical settings. Functional methods involve the use of sphere-fitting techniques. Developments of functional methods continue to reduce the error but both are still affected by a common issue of Soft Tissue Artifact. It is important to attempt to validate these methods in order to examine this relationship.

This study compares both predictive and functional methods with validation techniques such as ultrasound and MRI. It was found that all current methods and validation techniques are subject to errors, which means that there is, as yet, no quantifiable relationship between Soft Tissue Artifact and the HJC location. The most disturbing conclusion, however, is that the predictive methods that are favoured in clinical settings proved the least accurate.

CONTENTS

CHAPTER 1. INTRODUCTION	1
1.1. BACKGROUND	1
1.2. AIMS	3
CHAPTER 2. LITERATURE REVIEW	4
2.1. IMPORTANCE OF ACCURATE HIP JOINT CENTRE LOCATION (HJC)	4
2.2. BASIC ANATOMY OF THE HIP AND CONVENTIONAL AXIS SYSTEMS	4
2.3. METHODS OF LOCATING THE HIP JOINT CENTRE	6
2.3.1. PREDICTIVE METHODS	6
2.3.2. FUNCTIONAL METHODS	10
2.3.3. SPHERICAL ASSUMPTION	15
2.4. VALIDATION TECHNIQUES	17
2.4.1. X –RAY	17
2.4.2. ULTRASOUND	18
2.4.3. MAGNETIC RESONANCE IMAGING (MRI)	19
CHAPTER 3. METHODOLOGY	21
3.1. BACKGROUND	21
3.2. CHOICE OF ALGORITHM	22
3.2.1. MATLAB ALGORITHM	22
3.3. MOTION ANALYSIS SYSTEMS	23
3.3.1. VICON MOTION CAPTURE SYSTEM	23
3.4. DATA ACQUISITION	25

3.4.1. MECHANICAL MODEL TEST	25
3.4.2. SUBJECT TESTING	26
3.4.3. ULTRASOUND VALIDATION	28
3.4.4. PREDICTIVE VALIDATION	31
3.4.5. MRI VALIDATION	32
CHAPTER 4. RESULTS & DISCUSSION	33
4.1. MECHANICAL MODEL	33
4.2. SUBJECT TESTING	35
4.2.1. SUBJECT 1 – ORTHOGONAL AXIS	36
4.2.2. SUBJECT 1 – NON-ORTHOGONAL AXIS	38
4.2.3. SUBJECT 2 – ORTHOGONAL AXIS	39
4.2.4. SUBJECT 2 – NON-ORTHOGONAL AXIS	41
4.3. ULTRA SOUND VALIDATION	42
4.4. PREDICTIVE VALIDATION	46
4.5. MRI VALIDATION	49
4.6 RESULT COMPARISON	54
4.7 DISCUSSION SUMMARY	54
CHAPTER 5. CONCLUSION	57
CHAPTER 6. FUTURE WORK	58
REFERENCES	59
APPENDIX	62

CHAPTER 1. INTRODUCTION

1.1. BACKGROUND

Movement analysis of the human body is important in many industries such as sport, entertainment and medical diagnostic. Its uses in the medical field have grown over the years and have played a significant part in the development of medical technologies, diagnosis and rehabilitation procedures. One of the major forms of motion analysis used is *gait analysis*. This is the study of how people walk, and is used to determine spatial-temporal parameters and joint kinematics. Forces on joints can be calculated with reference to the reaction forces the patient applies to the floor during gait, however another main variable in this process is the accurate location of the joint centres. This is fairly straight forward with some joints, eg knee and ankle, but becomes more of a challenge when it comes to locating the Hip Joint Centre, which is located deep within the body surrounded by soft tissues such as muscle and fat. If both of these variables can be accurately obtained, this can result in identification and cause of pain in a particular area and any underlying problems like restrictions in motion, skeletal or joint misalignments and muscle weakness amongst others.

Many different methods have evolved throughout the years with the earliest relying on regression equations based on geometries of the pelvis and leg length to determine the location of the Hip Joint Centre. These equations proved to be inaccurate due to the fact that no two people share the same anatomical geometry. Leardini *et al* proved this in 1999 identifying errors of up to 38mm. Despite their errors in accuracy, regression equations are still being used in clinical environments

and pose a major concern if muscle forces and moments are being miscalculated by up to 20%.

In order to try and reduce these errors, more recently a number of 'functional' methods have been developed. All these methods assume that the hip joint is a 'ball and socket' joint where the centre of the femoral head is regarded as the joint centre, meaning the movement of the femur in relation to the pelvis could be modeled as a sphere. By attaching markers to the thigh of the subject and by circumduction of the leg, the trajectories can be mapped. The trajectories of each marker lie on the surface of concentric spheres and the location of the Hip Joint Centre is then calculated to be the average of all these centre points.

Functional methods show great advantages in Hip Joint Centre location due to their customizable nature, allowing them to overcome the issue of a subject's individual geometry. Although vast improvements have been recorded using functional methods to locate the Hip Joint Centre, they are still uncommon in clinical settings due to their high cost. (M.E. Harrington 2007) Though a major improvement in the results were found using the functional methods there are still significant errors present, the main cause being Soft Tissue Artifact (STA). Soft Tissue Artifact incorporates the movement of the soft tissues such as muscle, fat and skin in relation to the bone beneath. This is a problem in the functional methods, since the markers used to map the trajectories are attached to the outside surface of the skin, the movement of which is not synchronized with the bone underneath, causing the trajectories and the spheres modeled to not accurately represent the motion of the femur relative to the pelvis, thus providing additional inaccuracies to the joint's location.

1.2. AIMS

A previous study carried out in 2010 by Paul Byrne, predicted the location of the Hip Joint Centre through the use of motion analysis systems and complex algorithms. The aim of his study was to determine what effects STA has on the prediction of the Hip Joint Centre. It involved testing the proposed method on a mechanical model thus eliminating soft tissue artifact, and then using several external markers placed on the pelvis, femur and tibia of several subjects to examine what effect different angles of the knee and hip have on soft tissue movement of the leg. He then attempted to correct these STA errors by applying a compensation factor to the results obtained but was unsuccessful in determining any significant improvement in Hip Joint Centre location. This study was missing proper validation of the results since there was nothing to say whether the initial results were accurate or not.

This study will follow the initial stages of Byrne's attempts but differ by attempting to validate the results of a similar functional method through the use of ultrasound and MRI scanning. In addition to this, the results will also be compared to the predictive method proposed by Harrington *et al* (2007), which is perceived to be one of the most accurate predictive methods to date and to assess its accuracy in relation to problems presented by soft tissue artifact.

CHAPTER 2. LITERATURE REVIEW

2.1. THE IMPORTANCE OF ACCURATE HIP JOINT CENTRE LOCATION

The location of the Hip Joint Centre (HJC) is important in accurately determining the kinematics at the hip joint during gait analysis. Methods used up till now to locate the HJC have failed to do so accurately. In 2000, Stagni *et al.* examined the effects of ‘mis-location’ of the HJC. By quantifying how such errors propagate during gait analysis, the study identified errors of $\pm 30\text{mm}$ of the HJC. A ‘mis-location’ of 30mm anteriorly produced a propagated error in flexion/extension components of around -22%, similarly a ‘mis-location’ 30mm laterally resulted in errors of -15%. There was also a major error in the estimated stride time resulting in a mistaken location of 30mm posteriorly.

G Lenaerts *et al.* in 2009, similarly found it difficult to produce accurate locations of the hip joint. After carrying out studies on different subjects, using their individual geometry and comparing them to standard models, they recommended that for biomechanical analysis, more subject specific detail including bone geometry and musculature must be taken into consideration.

2.2. BASIC ANATOMY OF THE HIP & CONVENTIONAL AXIS SYSTEMS

The hip joint is an excellent example of a congruous joint. Having symmetrical concave and convex parts of both the acetabulum and femoral head representing the traditional ball and socket. Separating them is a pad of fibrous cartilage providing sufficient lubrication that allows for rotation around a fixed axis and simplifies muscle action on the joint. (F.H. Martini, 2008)

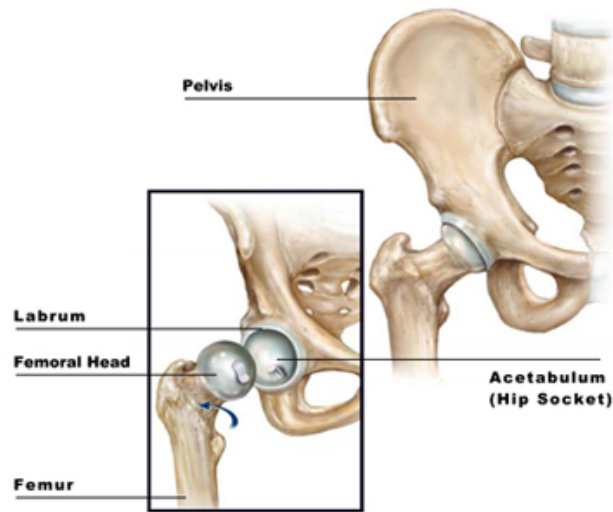


Figure 2.1 - Hip Joint Anatomy (www.bryankellymd.com)

Ge Wu produced the most commonly used axis system relating the pelvis to the femur in 2002. Based on earlier recommendations by Grood and Suntay in 1983, his study used the HJC as the point of origin for both pelvic and femoral axis systems, and in addition this Hip Joint Centre location was used to determine the proximal/distal (2nd) axis, relating it to the midpoint of the two femoral epicondyles as shown in the figure below.

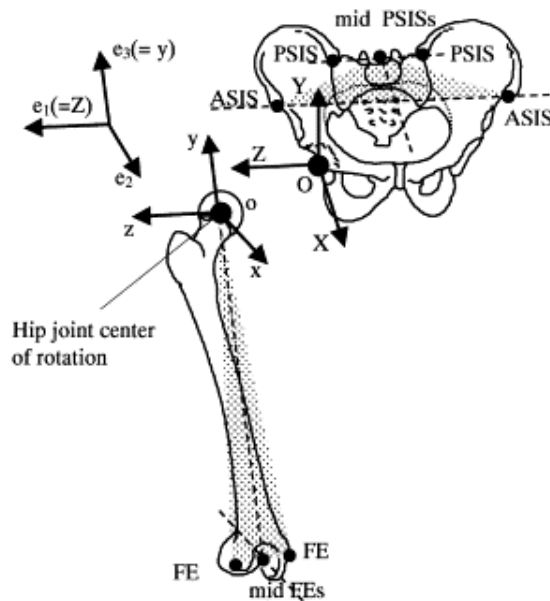


Figure 1.2 - Hip and Femoral Axis System (Wu, 2002)

2.3. METHODS OF LOCATING THE HIP JOINT CENTRE

Many methods have been produced for locating the HJC. These methods are split into two main categories – Predictive Methods and Functional Methods.

2.3.1. PREDICTIVE METHODS

Predictive methods use regression equations to accurately locate the HJC. These rely on factors such as pelvic geometry and leg length of the patient. In 1981, radiographic studies were carried out on 25 hip studies at the Newington Children's Hospital (NCH), Connecticut. These studies provided a model to determine regression equations based on their geometries. This model is shown below, where mean values of θ and β were found to be: $\theta = 28.4^\circ (\pm 6.6)$ and $\beta = 18^\circ (\pm 4)$, and the relationship C as a function of leg length was $C = 0.115L_{leg} - 0.0153$ (in metres). This was reported by Davis *et al* in 1991.

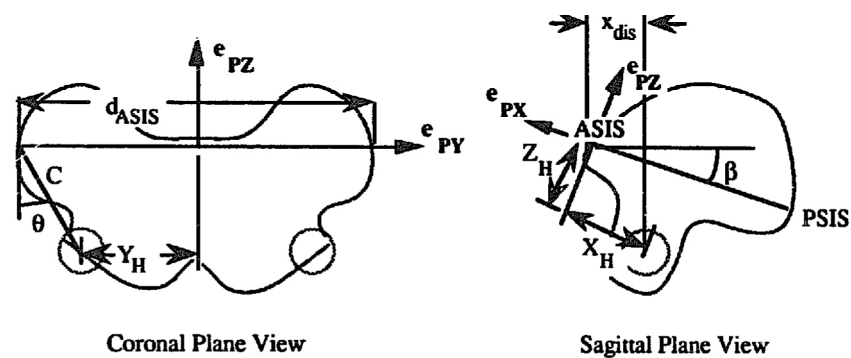


Figure 2.3 - Pelvic Geometry (Davis *et al.* 1991)

In 1999, Leardini *et al* compared these regression equations with ones developed by Bell *et al* in 1990. The difference between the two was that Davis *et al* incorporated both pelvic geometry and leg length into these equations whereas Bell *et al* relied solely on the pelvic width (PW). Another method mentioned in Leardini's

paper, was devised by Seidel *et al* in 1995, which produced more promising equations but was deemed not practical because it used the identification of an awkward pubic symphysis landmark. The main purpose of Leardini's test was to determine the accuracy of these methods, so Roentgen Stereophotogrammatic Analysis (RSA) was used to obtain the 'true' coordinates of the hip joint centre location. The regression equations produced from this study are shown below:

Bell's system: $x = -0.19PW$

$$y = -0.30PW$$

$$z = 0.36PW$$

Davis's System: $x = -0.95D + 0.031L - 4$

$$y = -0.31D - 0.096L + 13$$

$$z = 0.5PW - 0.055L + 7$$

As expected from these results, the Bell system provided less accurate results compared with Davis, producing low correlation factors of the x ($r = 0.21$) and y ($r = 0.34$) coordinates with the pelvic width.

As well as comparing these two methods they also compared them both with a functional method, involving a series of markers placed on pelvic and femoral landmarks, and their trajectories recorded. Combining the results from all 3 methods, it was found that the x -coordinate was best correlated with pelvic depth (PD), y -coordinate with distance between ASIS and hemolateral malleolus (L) and the z -

coordinate with pelvic width (PW). With this information they produced the following regression equations:

$$x = -0.31 PD$$

$$y = -0.096 L$$

$$z = -0.09 PW + 111$$

The results obtained from this test show that Bell's system was biased anteriorly in the x direction and superior in the y , relevant to the reference position. The Davis system was found to experience bias in all three axes, anteriorly, inferiorly and medially. The *root mean square value* is used as an indicator of the estimate accuracy. From these values it shows that the functional method is the more accurate. Both predictive methods were considerably different from the results produced with the RSA.

In 2007, Harrington *et al* compared the accuracy of Davis and Bell, along with a software recommendation from OrthoTrak (Motion Analysis Corp., CA, USA). As validation for these methods, Harrington used Magnetic Resonance Imaging (MRI) a more accurate method than the x-rays that were previously classed as the 'gold standard'. The MRI was used to test each method's effectiveness due to the fact that previous regression equations were based on adults, and it was feared that the errors produced would be amplified if used with children. Also tests were performed to determine if pelvic asymmetries affected the results. Locating landmarks such as the ASIS and PSIS along with the location of the Hip Joint Centre they were able to create a pelvis-embedded coordinate system with axis in accordance to the guideline produced by Wu in 2002.

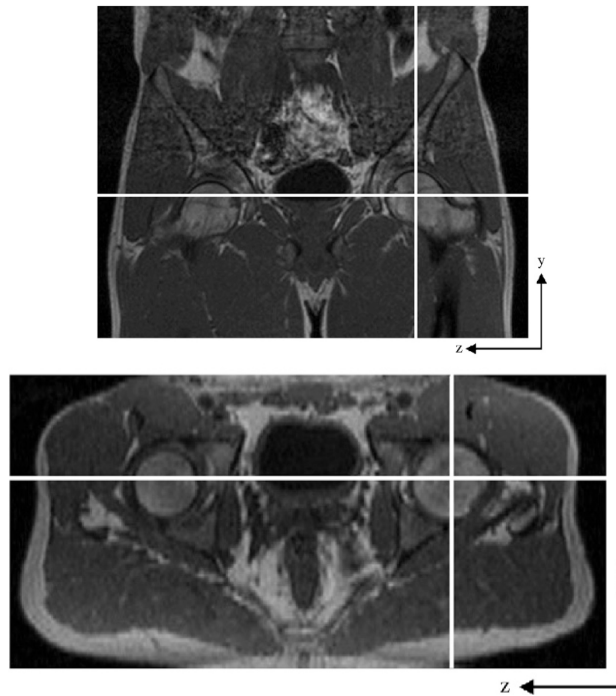


Figure 2.4 - MRI HJC location (Harrington et al, 2007)

After assessing the results of this study, Harrington *et al* produced their own set of regression equations for locating the HJC incorporating the variables that were attempted previously by Davis and Bell involving pelvic width (PW) pelvic depth (PD). These equations are displayed below.

$$\hat{x} = -0.24PD - 9.9$$

$$\hat{y} = -0.30PW - 10.9$$

$$\hat{z} = 0.33PW + 7.3$$

Note that these equations were developed for the location of the right hip for adults, children and young patients with spastic diplegic cerebral palsy. It was said that these new equations could improve the accuracy of HJC location by up to 7mm compared to previous regression equations. These do not take into consideration the

pelvic asymmetry, marker placement errors or soft tissue artifact. However, in a clinical environment these equations are found to be the most accurate to date. (M.E. Harrington, 2007)

2.3.2. FUNCTIONAL METHODS

The development of new ‘functional’ methods has overcome some of the drawbacks that were found using the predictive methods by being suited to each individual resulting in a reduction in location error. Predictive methods (whilst being the oldest) are still being used widely in many clinics worldwide because the newer functional methods necessitate the use of expensive equipment and software and involve complex algorithms meaning that patients with asymmetrical and deformed pelvises are not catered for. (M.E. Harrington 2007) Fortunately the development of these functional methods has not been sidelined and work is continuing to refine procedures and methodology, producing increasingly accurate results.

The idea of functional methods was first described by Aurelio Cappozzo in 1984, summarized by Leardini *et al* (1999) which suggests that the hip joint centre is the ‘pivot point’ of movement of the femur in relation to the pelvis. Leardini proved this to be much more accurate than the regression equations produced by Bell and Davis, by reducing bias and RMS errors.

This idea of the HJC acting as the pivot point, was the basis for many new developments in HJC location. This thesis will examine two of these, that of Halvorsen *et al* (1999) and that of Gamage and Lasenby (2002).

Halvorsen *et al* created the first in 1999, which incorporated Cappozzo’s idea. It was proposed that for the spherical joint, only three non-parallel and non-planar

displacements were needed to find its centre of rotation. If a body is circumscribed, the points on that body would lie on the surfaces of concentric spheres each with a radius equal to the distance to the centre of rotation. Similar to finding the axis of rotation, for the centre of rotation all point paths are segments of spheres rather than circles, each spherical displacement is perpendicular to the line connecting the centre of rotation and the midpoint of the displacement.

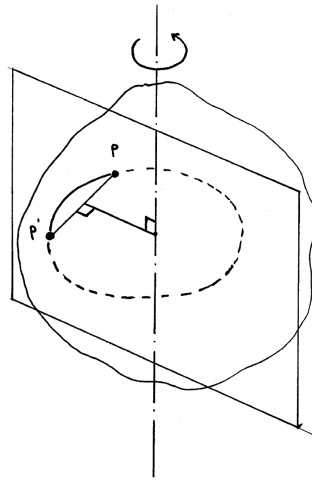


Figure 2.5 - Rotating Body

This means that the centre of rotation can be calculated knowing the angle of circumduction of the body and minimizing the loss function by taking the sum of squares. Where p_i represents the starting point, p_i' is the end point of marker i 's trajectory and q is the position vector of the centre of rotation.

$$s_2 = \sum_i \left(\Delta p_i^T \left(\frac{p_i + p_i'}{2} - q \right) \right)^2$$

This study proved that previous methods such as those carried out by Woltring in 1990, where Instantaneous Helical Axis (IHA) were used were deemed impractical because of high error sensitivity when skin tissue was added. This new method was found to be less affected by skin tissue artifact because it does not make assumptions about the rigidity of the body. This optimization method is named the *least squares method* and provided linear optimization algorithms making Halvorsen's method a lot simpler to apply than those of Woltring.

Gamage and Lasenby developed the second method in 2002. Their method involved a similar principle using the position of markers rather than the instantaneous trajectories to determine the location of HJC. They worked on the basis that a set of vectors on a body rotates round a time varying axis of rotation with a fixed centre of rotation with the tips of these vectors lying on concentric spheres. This idea based on marker positions required a frame rate to be selected so the position of markers were recorded at that point in time, where \mathbf{v}_k^p is the *p*th vector in the *k*th time instance. The centre of rotation *m*, and the sphere radius r^p

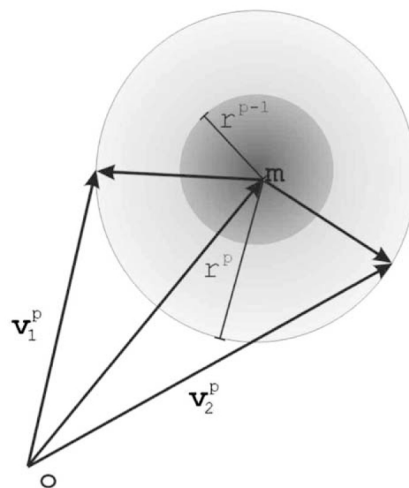


Figure 2.6 - Assumption of spherical marker movement in a ball joint (Gamage & Lasenby 2002)

From this information a *least squares cost function* can be given in the form of:

$$C = \sum_{p=1}^P \sum_{k=1}^N [(v_k^p - m)^2 - (r^p)^2]^2$$

This equation assumes there are P markers and N frames, where the P vectors are not assumed to have the same rotation because they are not connected by a rigid body but *do* share the same centre of rotation. Using the combination of equations regarding r^p and the differentiating vector, m results in the following equations for locating the centre of rotation:

$$Am = b$$

where;

$$A = 2 \sum_{p=1}^P \left[\left\{ \frac{1}{N} \sum_{k=1}^N v_k^p (v_k^p)^T \right\} - \bar{v}^p (\bar{v}^p)^T \right]$$

$$b = \sum_{p=1}^P [(\bar{v}^p)^3 - \bar{v}^p (\bar{v}^p)^2]$$

This produces a closed for solution and requires no ‘tuning’ parameters. This method although based effectively on the same principles as the Halvorsen method, calculates the centre of rotation using all the data gathered at the same time rather than calculating an average for each marker. Cereatti proved in 2004 that with a little modification to Halvorsens method, the cost functions of the modified method were equivalent to the ones proposed by Gamage and Lasenby and in doing so their solutions coincide, the errors of both being of similar magnitude.

However the method proposed by Gamage and Lasenby was not without its flaws. Even though it was superior to the Halvorsen method due to the fact that it did not require any manual adjustment of the unknown ‘optimal’ frame displacement, and can be used to find the instantaneous centre of rotation, it was still susceptible to inaccuracies.

Halvorsen proved that the results of Gamage and Lasenby were biased towards the centroid of each marker’s trajectory. On discovery of this, Halvorsen produced a bias compensation term solving it iteratively and incorporated it into their method relying on two important assumptions that the standard deviation of the noises is small compared to the trajectory radius and that due to large sample size, the average over the noise vectors is accurate. This new compensated method provided consistent estimates with better accuracy.

Camomilla *et al* in 2006, found flaws were still present in Halvorsen’s new compensated method and developed guidelines to be used to obtain the best results, including the recommendation that a range of movement of no lower than 15° and a minimum sample number of 500 should be used. During these tests however there was no error for soft tissue artifact taken into consideration, which is still thought to be the biggest cause of HJC ‘mis-location’.

Following a study of several of these functional methods in 2006, Rainald Ehrig *et al* developed another method expanding the principles of Schwartz *et al* in 2005. Schwartz *et al*, proposed a two-sided technique that involved the use of a local coordinate system on each limb and determined the centre of rotation as the point where the two rotation axes coincide, allowing for a non-stationary centre of rotation. Furthering this concept, Ehrig *et al* assume that the coordinates of the centre of

rotation must remain constant relative to both segments. This they called the Symmetrical Centre of Rotation Estimation (SCoRE). Again this method was tested with systematic and Gaussian errors, but soft tissue artifact was not included since it was assumed that it behaved as a rigid body structure. This method, however, performed more accurately than the other methods tested due to the low root mean square values produced. Despite its performance, due to its assumptions this method cannot be fully reliable.

The SCoRE method was later compared to the compensated Gamage and Lasenby method produced by Halvorsen in 2003. These tests were carried out on four adult cadavers to assess the accuracy in which the HJC could be located using stereophotogrammetry and also the effect that hip movement had on these results. The test involved using markers attached to cortical pins, which were implanted into the pelvis and femur along with 8 surface markers attached to the thigh. As a result of this testing it was found that the adapted Gamage and Lasenby method was still the most accurate. This study also concluded that the best results were obtained using the adapted Gamage and Lasenby algorithm with distal thigh markers and a wide range of hip movement. However there was found to be no relevant relationship between the magnitude of the soft tissue artifact and the errors in HJC location.

2.3.3. SPHERICAL ASSUMPTION

The functional methods described previously are all based on the same theory that for a body connected at one end by a spherical joint, all points on that body when circumducted would lie on the surfaces of concentric spheres sharing a common centre of rotation, thus being the hip joint centre. However it was only recently in

2010 that this was actually proved to be true. Cereatti *et al* conducted a study similar to that of their earlier one in 2009 where they attached intracortical markers to the bone eliminating the soft tissue artifact to determine the true motion of the bones beneath. This test showed that the movement of the bone did reflect that of a spherical joint producing 95% of predictions matching those of mechanical models. The theory that one of the causes of errors in these functional test were due to stereophotogrammic systems was deemed negligible, because these errors lie within range of the system's inherent limitations, meaning that it would not be detected. They concluded that the acetabulofemoral joint can be modeled as a perfectly spherical joint within the movement limitations of 20° to 70° flexion/extension, 0° to 45° abduction/adduction and 0° – 30° internal/external rotation.

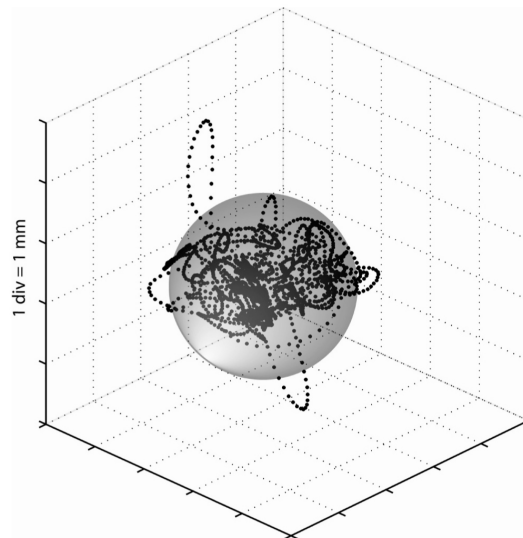


Figure 2.7 - Trajectory of Hip Joint Centre relative to the pelvis (Cereatti et al, 2010)

The figure above shows the results from this test displaying that 95% of the hip joint centre trajectories lie within the 1.5mm radius. Note that if this were a perfectly spherical joint then the radius of the sphere containing 95% of the trajectory would be zero.

These small errors could be a result of movement of the femoral head within the acetabular socket. An example of this movement is posterior anterior glide. This has been fairly neglected in terms of research, however one study by Harding *et al*, carried out tests on cadaveric specimens to determine whether posterior/anterior glide was actually present in the hip joint. Up until 2003 it was only a theory until the study showed that posterior/anterior glide was present in all specimens tested. Even though it was found to be present in these tests, there is insufficient evidence to say that it has any sufficient effect on HJC location predictions and will require further investigation.

2.4. VALIDATION TECHNIQUES

It is important for the location of the HJC to be accurate, however in clinical settings, the use of regression equations and gait analysis systems are cumbersome enough without having to try and prove that the hip is located where you say it is. It is necessary for these different methods to be validated before being put into clinical use.

There are many ways to see inside the human body, this section will discuss some of the different types of imaging techniques that could be used in locating the HJC.

2.4.1. X-RAY

The first thing that many people would think of when asked about how we see inside the body would be x-rays. A German scientist called Wilhelm Conrad Roentgen, in 1895, first documented x-rays, which are a form of electromagnetic

radiation. They can easily pass through tissues due to their short wavelength and high-energy electrons. The body is made up of a variety of different tissues of different densities, for example bone is denser than muscle. The denser the tissue is the fewer x-rays can pass through. It is the blockage of these rays that make up the x-ray image. A special x-ray film is placed behind the subject and the silhouette of the different tissues is produced. X-rays were considered the ‘gold standard’ and have been used in studies performed by Bell *et al* (1990) and Leardini *et al* (1999) to validate their predictions of the HJC locations. However this method involves exposing the subject to small amounts of radiation that can have long term damaging effects on tissues in the body. (M.E. Harrington 2007)

2.4.2. ULTRASOUND

Ultrasound uses high frequency sound waves to produce an image of the inside of the body. Like x-rays, it relies on the density of tissue to produce a clear picture; it works by the detection of the reflected ultrasound waves as they hit the surface of a tissue. The denser the tissue the more sound waves will be reflected back and detected by a sensor. This method is commonly used throughout the medical field for many purposes. It can be used to examine pregnancies, heart function and blood flow. However this system does have its limitations, since the deeper they travel the more the sound waves are absorbed by their surroundings therefore producing a weaker image.

In 2005, Hicks *et al* used ultrasound to validate sphere-fitting methods to determine their clinical applicability. A linear probe operating at 10MHz was positioned on the frontal plane and images taken in both horizontal and vertical

orientation to determine the position of the femoral head. However it was found that it was difficult to determine the exact centre of the femoral head using this method.

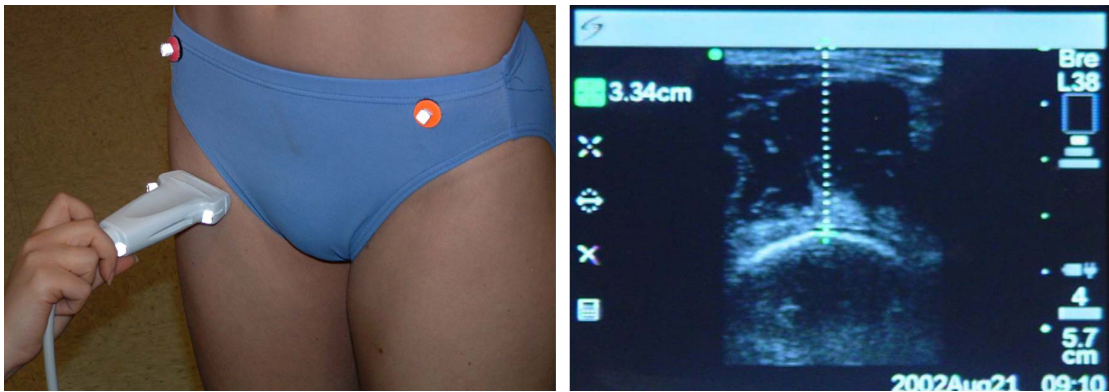


Figure 2.8 - Ultrasound Procedure (Hicks et al, 2005)

2.4.3. MAGNETIC RESONANCE IMAGING (MRI)

Magnetic Resonance Imaging uses a strong magnetic field and radio waves to produce ‘sliced’ images of inside the body. A strong magnetic field lines up all the protons that are inside the hydrogen atoms inside the body. Radio waves are then pulsed into the body knocking these atoms out of the way. Once the radio waves stop the protons then move back into their initial position and in doing so emit radio waves themselves. These waves are then detected by a scanner and an image is recreated. The protons of different tissues in the body return to their position at different speeds allowing the tissue density to be determined by the amount of signals emitted. A number of slices can be produced during one scanning session; these can then be processed to produce a detailed 3D image of the body, allowing for easy examination.

MRI imaging has been used extensively in determining the joint kinematics of the human body. Harrington *et al* used MRI in 2007 to validate their new regression equations with good results. Following Harrington’s success, Heller *et al* (2007) used

this technique when developing a new model for human knee kinematics. Using 3D modeling packages, overlaid onto the MRI images, they were able to produce a full 3D model of the knee joint and examine in detail its kinematic properties.

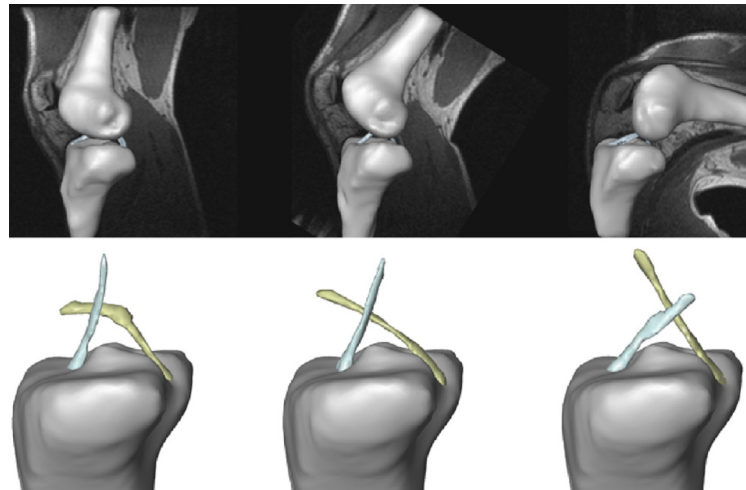


Figure 2.9 - MRI with Overlaid 3D model (Heller et al, 2007)

This method is not only used for lower limb kinematics; in 2009 magnetic resonance imaging was used to validate the location of the glenohumeral joint centre against other established techniques by Campbell *et al* (2009). This study used external markers around the shoulder, which were tracked using medical imaging software ‘Mimics’ with great success.

CHAPTER 3. METHODOLOGY

3.1. BACKGROUND

Many studies have been carried out to resolve the problem of accurately determining the location of the Hip Joint Centre. Initially, regression equations were used based on the patient's geometry involving pelvic width, depth and leg length. However it can be seen that these equations are known to be highly inaccurate due to the vast differences in individual body parameters, and therefore cannot be used for the entire population. These equations also assume symmetry of the pelvis, which is highly unlikely to occur in practice, even more so if the subject suffers from pelvic deformities resulting in gait abnormalities, requiring gait analysis to be carried out. This shows that these equations should not be assumed as accurate in these situations.

The developments of functional methods have produced results with greater accuracy but are also subject to error. The sphere fit method described in chapter 2, provides a logical underlying principal that if a limb is circumducted, all points on that limb will lie on the surface of a respective sphere each sharing the centre of rotation, in this case the HJC. Although improvements have been made, the complication of soft tissue artifact remains the main cause of error for each of these methods.

This study will assess the accuracy of functional and predictive methods by using the different validation techniques that have previously been used to determine the HJC location such as ultrasound and MRI, thus identifying the possible cause of errors experienced by each.

3.2. CHOICE OF ALGORITHM

As discussed in chapter 2 there have been many variations of functional methods used to try to more accurately locate the centre of rotation of a ball joint with varying degrees of success. From this research, the preferred method used for this study was the compensated version of the Gamage and Lasenby method. However, this compensated adaptation uses iteration which would therefore increase its complexity. So because of this the original method proposed by Gamage and Lasenby will be used. This involves using the trajectory of individual markers and applying a *least squares* method between the radius of the marker trajectory and the distance from each marker to the HJC. The purpose for the compensation by Halvorsen was to reduce the bias that this method showed, however since this study looks into the influence of STA, this bias should not have an affect on the results of this study.

3.2.1 MATLAB ALGORITHM

In order to be able to process the data collected from the VICON system, a MATLAB program was created based on the Gamage and Lasenby algorithm. This program was written to validate the algorithm based on data collected using a mechanical model. MATLAB uses the coordinates of three markers located on the hip section to determine a local coordinate system for the model. The trajectories of the leg markers are then transformed into the newly determined system. The program then determines where these markers are in relation to the HJC. Using the coordinates of these instantaneous points, the program is then able to determine an average centre of rotation common to all points along the markers' trajectories. This

then outputs the predicted HJC coordinates relative to the origin of the local coordinate system - in this case the first hip marker. The program also examines the uncertainty of this method by calculating the *bias* and *root mean square values* for each test. These values are unlikely to be accurate but will give an idea of what is expected in the subject tests. This program is then adapted keeping the basic principles of the Gamage and Lasenby method, adding an additional hip marker generating the approved axis system proposed by Wu (2002). The MATLAB code for both mechanical model and subject testing are located in the APPENDIX.

3.3. MOTION ANALYSIS SYSTEMS

Motion analysis systems are used in various industries including sport, entertainment and medical fields. These systems take many forms from human activity recognition, human motion tracking and motion analysis of body parts. In the medical field, the advance in technology of these motion analysis systems has been of great benefit. Gait analysis has been around for a long time and is used in the medical field to identify walking abnormalities and related problems in patients so that they can be treated effectively. Gait analysis systems can record a number of different parameters such as spatial-temporal parameters (step length, width and walking speeds etc.), and more relevant to this subject, kinematic parameters such as joint movement/rotation and the angles the joints are positioned.

3.3.1. VICON MOTION CAPTURE SYSTEM

The tests are to be carried out using a VICON motion capture system. This system works by using 12 infrared (IR) cameras positioned around the laboratory, whose

light is reflected off small reflective markers positioned on the subject at specific locations. Each individual camera then detects the reflected signals and their location recorded in each camera's 2 dimensional plane view. Due to the number and location of these cameras, it is possible to combine the data from each and triangulate each marker's location in 3 dimensional space with very little error. Using the Nexus software package along with this system allows the labeling of each individual marker and allowing its position to be recorded over time. The layout of the camera position in the laboratory is provided below.

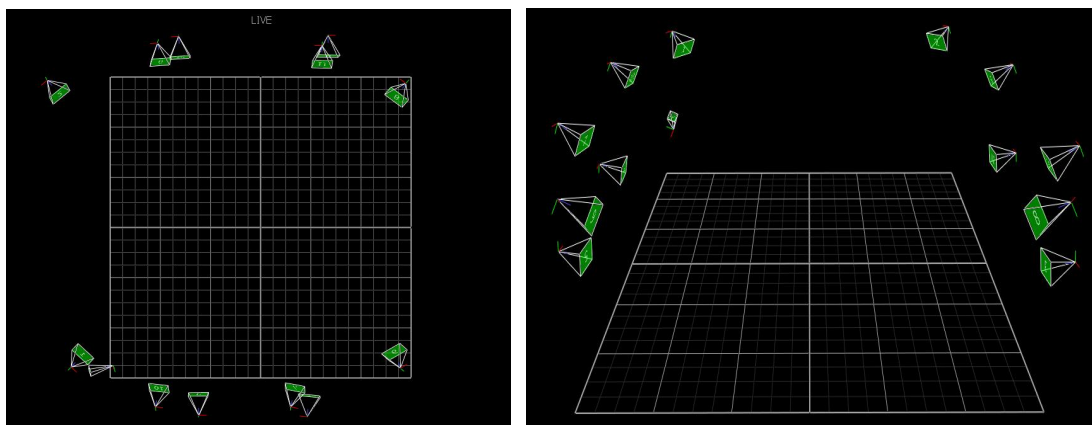


Figure 3.1 – VICON Lab Layout

VICON system first needs to be calibrated in order to obtain accurate results. The calibration of this system requires both dynamic and static calibration. Firstly the system is calibrated dynamically. This is done using a calibration wand. This wand has 5 small reflective markers, 3 of which are attached non-collinearly. This wand is then waved around the working volume required for the test until all cameras have sufficient information. The system, knowing the geometry of the wand and its markers, can then verify the location of each camera. Once this is completed successfully the system is then statically calibrated by placing the calibration wand in

the centre of the room allowing it to establish the origin of the global coordinate system. This system is set up to record the coordinates of individual markers at a rate of 100Hz.

3.4. DATA ACQUISITION

The data for both of the tests proposed (mechanical model and subject tests) was obtained using the VICON system described in chapter 3.2.1. This system used IR cameras to record the trajectories of several markers located on both hip and leg. This data was then exported as a .csv file for further analysis.

3.4.1. MECHANICAL MODEL TEST

In order to validate the algorithm for this study, a basic mechanical model was created to represent the ‘perfect’ hip joint. It consisted of a ball joint connected to a metal rod with a number of pins extruding from it to distance the markers from the rod. This then simulates the test carried out on cadavers undertaken by L Harding *et al* in 2003 where they used intercostal pins to attach the markers thus removing the effects of any soft tissue artifact.

The model was attached to a stand for stabilization. This wasn’t compulsory, as the algorithm does not require the axis system to remain stationary, however the added stabilization was more practical and benefited the test procedure. The model was split into two segments, the ‘hip’ and the ‘leg’. 3 markers were attached to the hip in order to determine a local coordinate system, and 4 markers attached to different locations on the leg. The model was then positioned in the centre of the lab and circumduction of the leg carried out. The trajectories of the markers were

recorded for use in the algorithm. An image of this mechanical model is shown in the figure below alongside a screenshot of the visible marker segments detected by the VICON system.

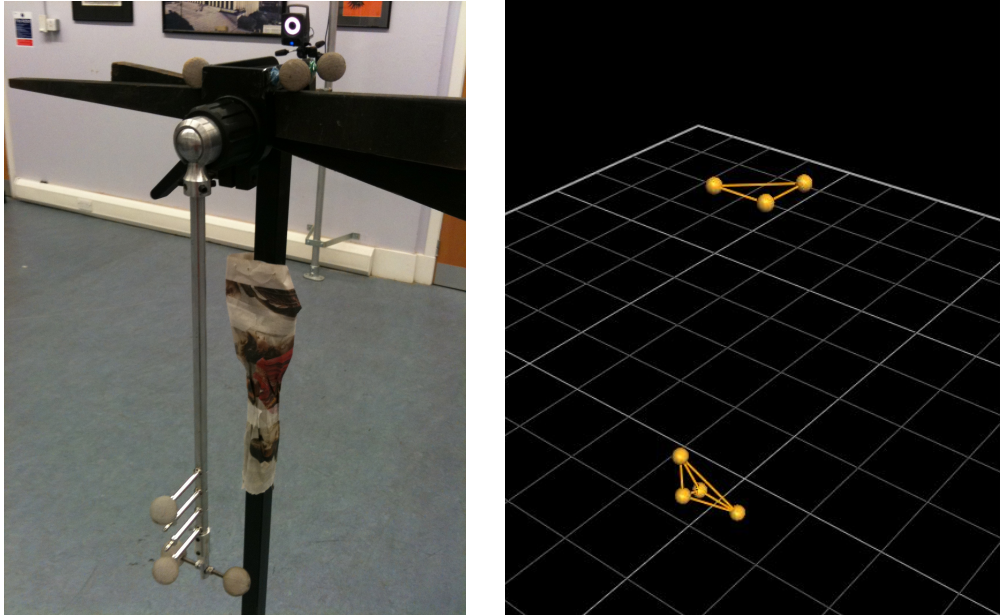


Figure 3.2 – Mechanical Model and Nexus Screenshot

3.4.2. SUBJECT TESTING

In contrast to the mechanical model, the hip area of the test subjects consisted of various amounts of soft tissue artifact. It was important then to determine a local coordinate system that would be least affected by this issue. The most commonly used axis system for this type of study is the one proposed by Wu (2002), which used the bony landmarks of the pelvis because they are fairly easy to locate and have relatively low soft tissue artifact. Taking this into account, reflective markers were positioned on each Anterior Superior Iliac Spine (ASIS) and Posterior Superior Iliac Spine (PSIS). These were then used to determine the local coordinate system.

During Byrne's study, he used 8 markers on the right leg, 4 on the thigh, 1 on each femoral epicondyle and 2 on the anterior of the tibia. This was because he was determining what effect knee flexion had on soft tissue artifact, however his results showed that there was very little change in the marker positions on the femoral epicondyle and tibia markers so they will not be used in this study. Therefore, 4 markers were positioned on the right thigh, 2 laterally and 2 anteriorly, all different distances down the length of the thigh. A summary of these marker positions is shown below.

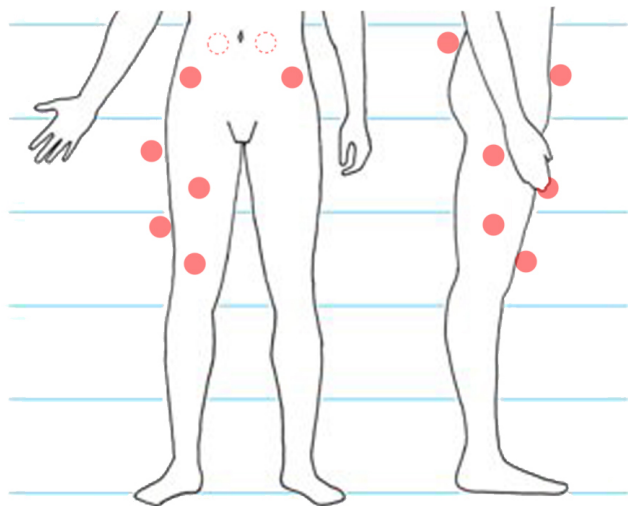


Figure 3.3 – Subject Marker Positions

Once the markers were attached, the subject was then positioned in the centre of the laboratory and a static calibration of his position was carried out in order to label the markers correctly and generate the appropriate segments. The subject was then asked to perform a circumduction of the right leg. The VICON system tracked all 8 markers over 2000 frames. The markers' instantaneous coordinates were recorded and exported.

This procedure was carried out on 2 subjects.

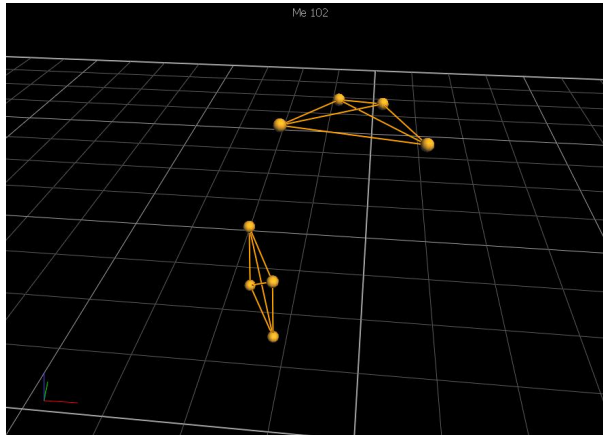


Figure 3.4 – Nexus Screenshot showing pelvis and thigh markers and segments

3.4.3. ULTRASOUND VALIDATION

To properly assess the effects of soft tissue artifact during the subject testing it is important to know the true location of the HJC. This can be done using technologies such as x-rays, ultrasound and MRI. There are drawbacks concerning all three methods. Whilst x-rays provide clear decipherable images, beneficial to this study, they involve exposing the subject to harmful x-rays, so this method was avoided. Ultrasound and MRI were chosen due to their harmless nature and ability to produce clear images. MRI would provide the best images being easily manipulated in 3D software packages to obtain the coordinates of the HJC in relation to a defines axis system.

In order to determine the HJC using ultrasound it was initially intended to place the ultrasound sensor on the ASIS to determine the true distance from it to the HJC. This was unsuccessful because the ultrasound machine used would only produce images 110mm deep, deteriorating in picture quality at around 60mm, which didn't provide a clear image of the hip joint from that angle. In order to get round this problem, it was found that the best position for the sensor to detect the hip joint was

horizontally from the frontal plane. This produced a clear image of Subject 1's hip joint.

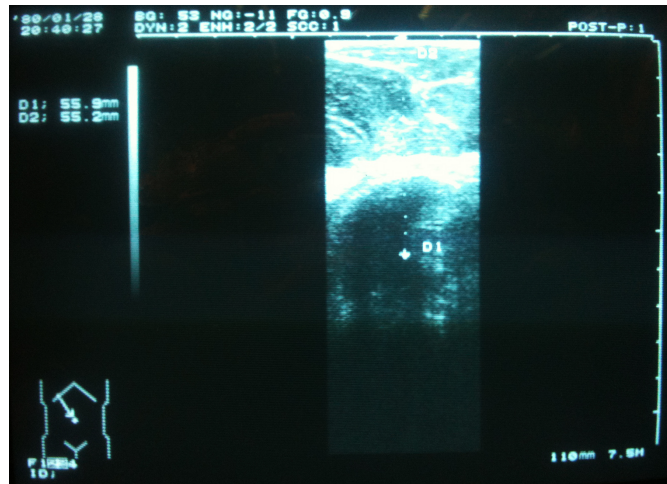


Figure 3.5 Subject 1 – Ultrasound

Markers were then placed manually on the image indicating the surface of the body and the centre of the femoral head, giving the distance between the two, This was done three times and an average taken to reduce the human error in onscreen marker placement. It was found that for Subject 1 the hip joint centre was located 55.4mm from the anterior of the body. Once this had been determined there was the problem of relating it to a local coordinate system for comparison to the MATLAB results. Assuming that the scanner was in the same frontal plane as the ASIS, this would be the best point of reference. Lines were drawn on the subject and the centre of the scanner and the right ASIS marked. To provide scale a rule was placed next to the area and photographed. This would provide dimensions in the other axis to determine a 3 dimensional coordinate for the HJC using the ASIS as the origin. This would obviously have some inaccuracies due to human error but would provide a reasonable guideline for the purposes of this study.

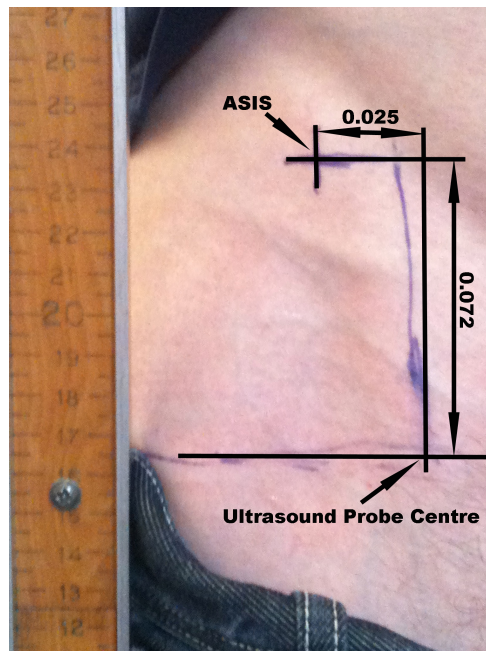


Figure 3.6 – Subject 1 Photo (Dimensioned in Photoshop)

When this procedure was repeated for Subject 2, the scanner was unable to produce a clear image of the femoral head. This could be because his hip joint was located outside the range of the scanner thus failing to be detected. There was however a significant arc at around 65mm below the surface. This was assumed to be the surface of the femoral head and estimation for its centre was noted.

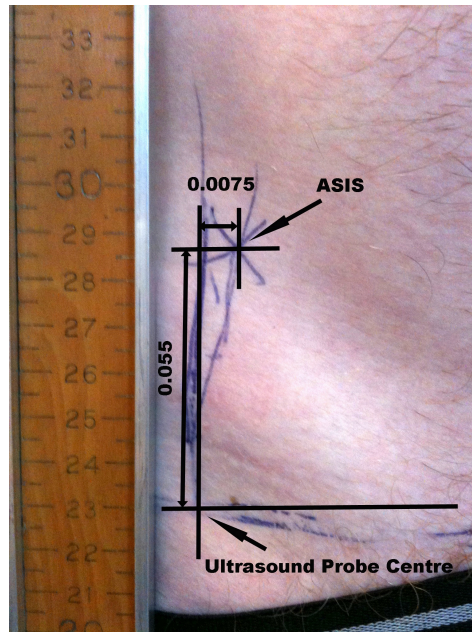


Figure 3.7 – Subject 2 Photo (Dimensioned in Photoshop)

Due to this uncertainty, Subject 1 will be used as the main test. If the results of Subject 1's proved to be accurate with MATLAB, then MATLAB results for Subject 2 would be used to determine if what was perceived to be the surface of the femoral head was in fact true.

3.4.4. PREDICTIVE VALIDATION

It is important to attempt to validate the results obtained from functional testing with a predictive method. This is because predictive methods are still the main methods used in clinical settings to locate the HJC. For this reason, validation of these functional tests were carried out using the regression equations suggested by Harrington *et al* (2007). From their studies, these equations have been proven to give the most accurate results for predictive methods and were validated themselves through the use of MRI. These equations require the variables Pelvic Width (PW) and Pelvic Depth (PD) to produce the coordinates of the Hip Joint Centre. For this

reason the data from the VICON system was examined and used to calculate these variables for each test subject. This form of validation was also carried out on Byrne's subjects to determine if his predictions were correct.

3.4.5. MRI VALIDATION

The best form of validation for functional methods is through the use of MRI. This has proved in the past to be the most accurate form of imaging technique to locate the HJC. It is important for the MRI scan that the correct coordinate system is used in order to compare the results effectively. To achieve this, cod liver oil capsules were positioned on the bony landmarks of the pelvis (ASIS and PSIS) which were then used to form the local coordinate system produced by Wu (2002) thus allowing for the best comparison of the various results whilst keeping the local coordinate system consistent throughout all methods of validation.

CHAPTER 4. RESULTS & DISCUSSION

4.1. MECHANICAL MODEL

The purpose of the mechanical model test was to validate the use of the MATLAB algorithm based on the functional method proposed by Gamage and Lasenby (2002).

The test results showed the location of the computed centre of rotation in relation to the hip markers (c), the individual spherical radii for each of the thigh markers and the three hip marker trajectories. These results are shown below.

$$c = \begin{bmatrix} 42.75 \\ -71.44 \\ -45.80 \end{bmatrix} mm$$

Radii of thigh markers: Mk1 = 331.04mm

Mk2 = 405.83mm

Mk3 = 463.56mm

Mk4 = 464.05mm

As you can see from the image of the mechanical leg in Figure 3.2 in section 3.4.1, Mk3 and Mk4 appear to be equidistant from the centre of rotation of the leg. The intention was to try and position these markers exactly the same distance from the centre, however the results show a slight difference in these measurements highlighting the fact that any slight error in marker positioning can have an effect on the final outcome of the test.

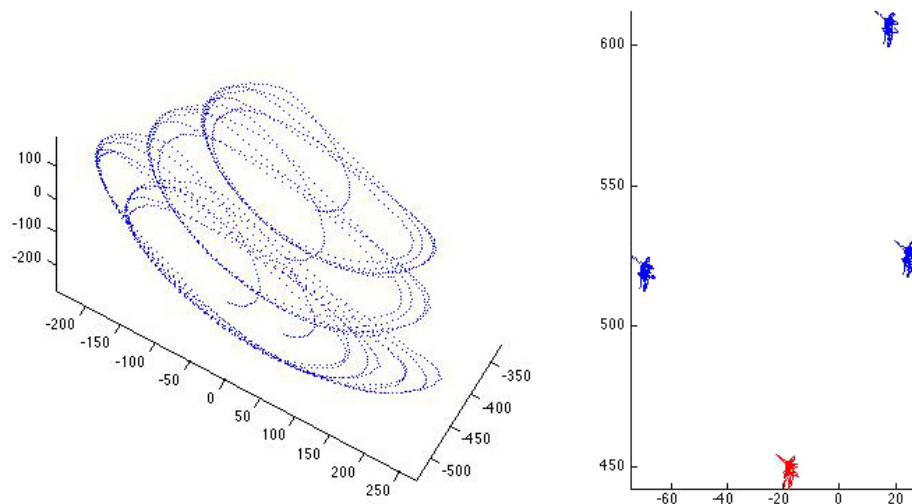
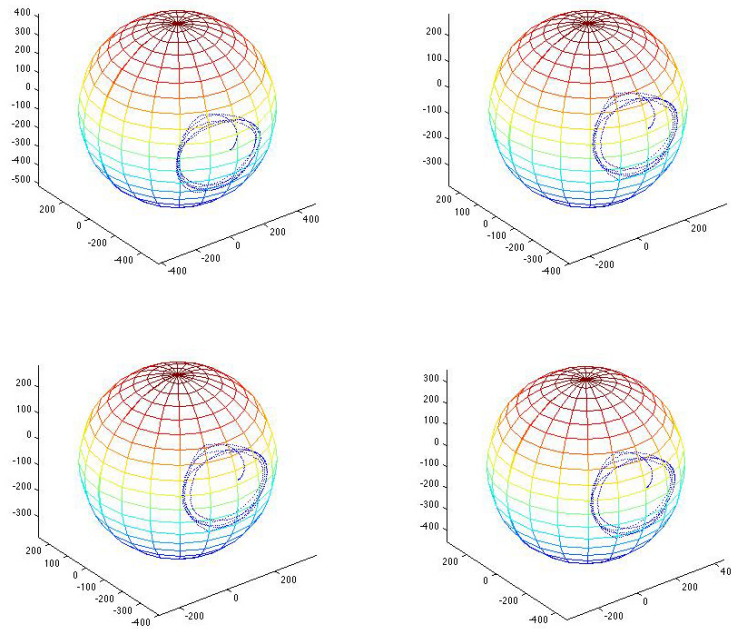


Figure 4.1 - Thigh and Hip Marker Trajectories in Global Coordinate System
(all Axes in mm)

The figure above shows the trajectories of the thigh and hip markers in the global coordinate system, which ensured that the data exported from the Nexus software was correct. Each individual trajectory can be seen clearly.



**Figure 4.2 - Marker Trajectories on their Relative Spheres in Local Coordinate System
(all Axes in mm)**

Figure 4.2, shows each individual marker trajectory on the surface of its individual sphere, each of the spheres having a common centre of rotation. The bias for each of the individual markers has an order of magnitude of 10^{-4} or smaller and the *root mean square error (rms)* of each marker is 0.5mm or less. These results compare well with the *rms* values found by Cereatti *et al* (2009), who did a similar experiment reducing the STA by using intercostal pins achieving *rms* error values of 0.3mm or less. [18] This shows that the Gamage and Lasenby (2002) algorithm works well and can therefore be used for data analysis of the subject tests.

4.2. SUBJECT TESTING

After finding that the MATLAB algorithm was successful with the mechanical leg model, it could then be applied to the data collected for the subjects. Even though the MATLAB code had to be modified to accommodate the new local coordinate

system, it was set to produce the same outputs as the mechanical model. However, in the subject testing, the local coordinate system proposed by Wu, assumes orthogonal axes, however in practice this may not be the case due to some pelvic asymmetries. Therefore a test was carried out using an orthogonal local coordinate system and repeated with the coordinate system without Wu's assumption to examine the differences. In addition to these changes, instead of positioning the origin at the centre of the pelvis as Wu described in 2002, the origin of the local coordinate system was located at the right ASIS so it could be validated using ultrasound testing. These results were then converted back into the general coordinate system for further validation techniques.

The results for both subjects are shown below.

4.2.1. SUBJECT 1 – ORTHOGONAL AXIS

$$c = \begin{bmatrix} -36.10 \\ -123.20 \\ -27.43 \end{bmatrix} mm$$

Radii of thigh markers: Mk1 = 139.97mm

Mk2 = 199.19mm

Mk3 = 273.31mm

Mk4 = 337.86mm

The radii of the thigh markers were averaged over the entire trajectory. In closer examination of the points, the largest differences between the maximum and minimum radii are 19.02mm and 21.76mm experienced by markers 2 and 4

respectively. These are the two markers positioned on the anterior of the thigh and are clearly affected more by Soft Tissue Artifact (STA), perhaps this is because there is more present at the anterior of the thigh.

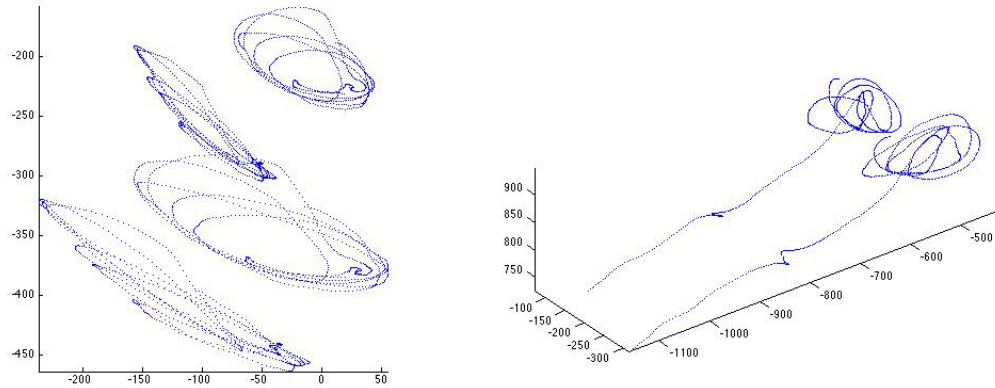


Figure 4.3 - Subject 1 - Thigh and Hip Marker Trajectories in Global Coordinate System (all Axes in mm)

The figure above resembles that of the mechanical model, displaying the trajectories of the individual thigh markers in the global coordinate system. The second image differs slightly displaying only 2 of the hip markers in the global coordinate system for reasons of clarity. They also show a lot more natural motion in the pelvis when performing the circumduction compared to the relatively still mechanical model.

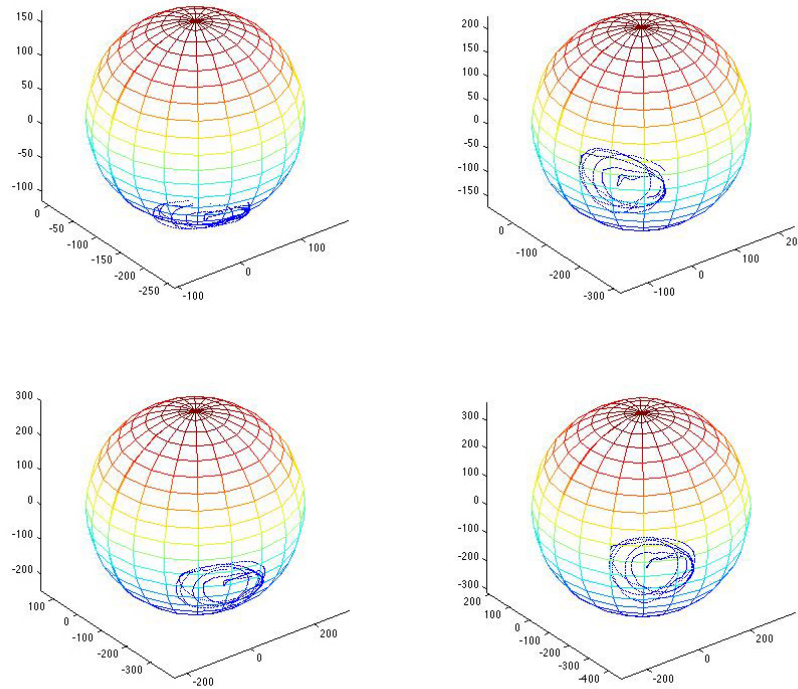


Figure 4.4 - Subject 1 - Marker Trajectories on their Relative Spheres in the Local Coordinate System (all Axes in mm)

The figure above conforms to that of the mechanical model, displaying the trajectories of the individual thigh markers on their relative spheres, each sharing the same centre of rotation.

4.2.2. SUBJECT 1 – NON-ORTHOGONAL AXIS

Below are the results from the algorithm without using orthogonal assumption.

$$c = \begin{bmatrix} -36.49 \\ -122.32 \\ -28.11 \end{bmatrix} mm$$

Radii of thigh markers: Mk1 = 141.02mm

$$Mk2 = 200.10\text{mm}$$

$$Mk3 = 274.34\text{mm}$$

$$Mk4 = 338.83\text{mm}$$

These results show that if a truly orthogonal axis is used then the results differ in both predicted HJC location and predicted radii of the spheres by a maximum of 1.05mm for Subject 1.

4.2.3 SUBJECT 2 – ORTHOGONAL AXIS

The results for Subject 2 using the orthogonal local coordinate system are shown below.

$$c = \begin{bmatrix} -90.83 \\ -93.58 \\ -31.47 \end{bmatrix} \text{mm}$$

Radii of thigh markers: $Mk1 = 161.95\text{mm}$

$$Mk2 = 209.25\text{mm}$$

$$Mk3 = 262.36\text{mm}$$

$$Mk4 = 314.76\text{mm}$$

Again in closer examination of the radii for each of the points along each marker's trajectory, it can be seen that markers 1 and 2 experience the widest range of radii. This shows that STA was more prominent at the top of the thigh where these markers were positioned, which demonstrates the point that STA effects are unique to each individual subject.

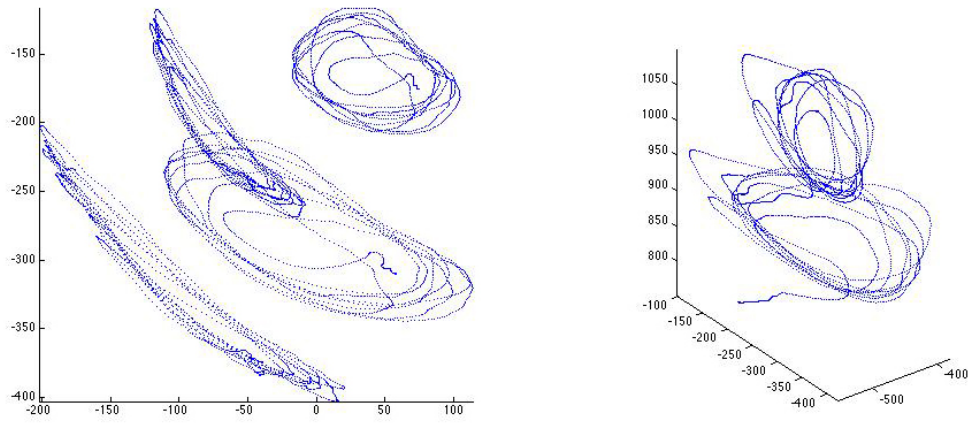


**Figure 4.5 - Subject 2 - Thigh and Hip Markers in Global Coordinate System
(all Axes in mm)**

The figure above depicts the trajectories produced by the 4 thigh markers and 2 of the hip markers in the global coordinate system. It can be seen more clearly on this subject that the hip markers mapped out similar trajectories to the thigh markers when the test was carried out.

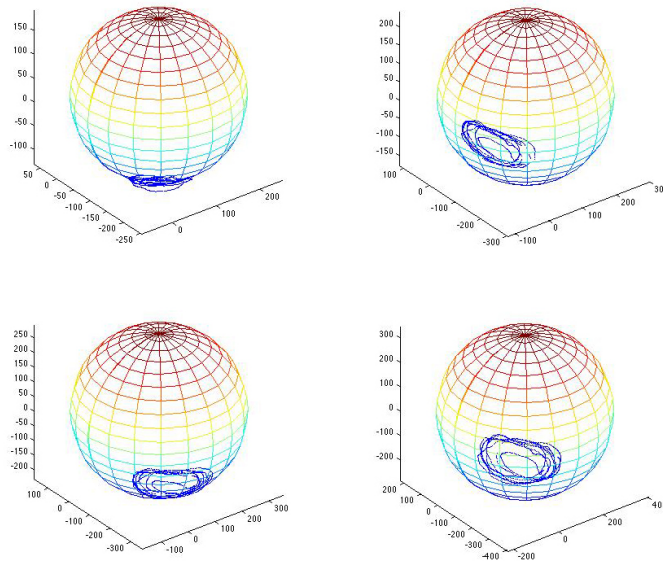


Figure 4.6 - Subject 2 - Marker Trajectories on their Relative Spheres in the Local Coordinate System (all Axes in mm)

4.2.4 SUBJECT 2 – NON-ORTHOGONAL AXIS

The computed centre of rotation and sphere radii for Subject 2 are shown below using the non-orthogonal axis system.

$$c = \begin{bmatrix} -92.95 \\ -90.23 \\ -31.15 \end{bmatrix} mm$$

Radii of thigh markers: Mk1 = 163.88mm

Mk2 = 213.00mm

Mk3 = 265.64mm

Mk4 = 318.95mm

The results obtained by removing the orthogonal correction in the MATLAB code shows the slight change in hip joint centre prediction with the y coordinate decreasing by 3.36mm. The mean radii for each thigh marker trajectory also increased significantly, marker 4 increasing the most by 4.1mm.

Both of these subjects were tested 3 times, each producing slightly different results. This could be due to unintentional changes in procedure so for this reason only the last test for each subject has been detailed.

4.3. ULTRASOUND VALIDATION

In order to validate both subjects' HJC location using ultrasound, its position had to be calculated using the data previously collected in section 3.4.3.

The measurements obtained from the ultrasound and photographs allow for the position of the HJC to be calculated using simple geometry. Below is a wire frame representation incorporating the data collected from the ultrasound and photographs for Subject 1.

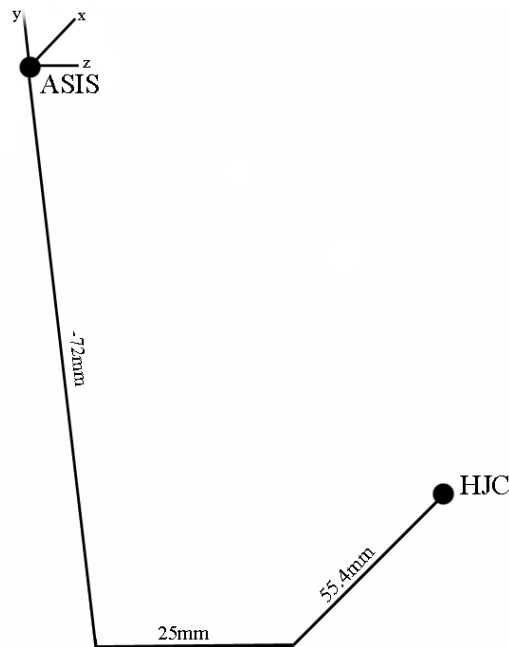


Figure 4.7 – Subject 1 - Wireframe of Ultrasound Positioning

From this diagram it can be said that the location of the HJC is:

$$c = \begin{bmatrix} -55.4 \\ -72 \\ -25 \end{bmatrix} mm$$

However, even though similar to the functional method using the ASIS as the origin, this result is based on an orthogonal axis in the frontal plane meaning the x axis is parallel to the ground, whereas the functional method uses a local coordinate system using the bony landmarks of the pelvis determining the x axis as the join of

the midpoints between the ASIS and PSIS, which is unlikely to be parallel to the ground. This coordinate can be transformed to the pelvic axis system by determining the angle of the pelvis as follows:

1) The midpoints of the two ASIS and PSIS had to be determined. Points were taken from initial marker positions from the functional method.

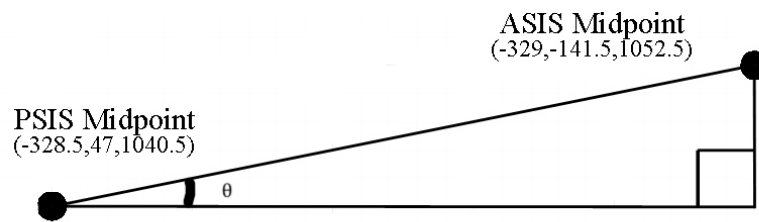
$$\begin{aligned} ASIS \text{ Midpoint} &= \left(\frac{207-451}{2}, \frac{-146-137}{2}, \frac{1013+1092}{2} \right) \\ &= (-329, -141.5, 1052.5) \end{aligned}$$

$$\begin{aligned} PSIS \text{ Midpoint} &= \left(\frac{284-373}{2}, \frac{46+48}{2}, \frac{1029+1052}{2} \right) \\ &= (-328.5, 47, 1040.5) \end{aligned}$$

2) The distance between the two midpoints, Pelvic Depth (PD):

$$\begin{aligned} PD &= \sqrt{\Delta x^2 + \Delta y^2 + \Delta z^2} \\ &= \sqrt{0.5^2 + 188.5^2 + 12^2} \\ &= 188.9mm \end{aligned}$$

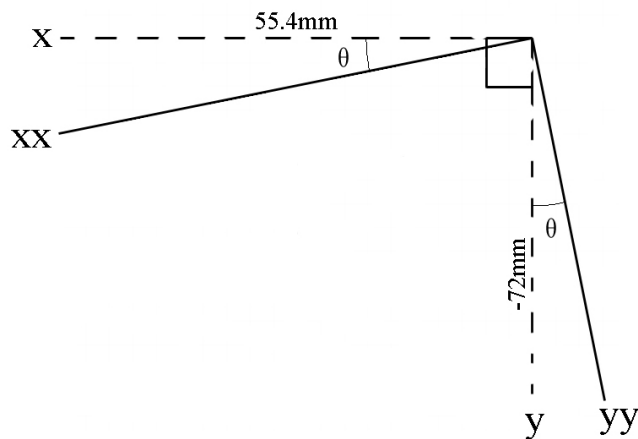
3) The angle of the pelvis (θ) could then be determined:



$$\theta = \sin^{-1} \left(\frac{12}{188.9} \right)$$

$$= 3.64^\circ$$

4) Knowing this angle allows the original axes (x, y, z) to be converted into the new axes (xx, yy, zz). The z coordinate remains the same due to rotation around z axis.



$$xx = \frac{55.4}{\cos 3.64}$$

$$= 55.51 \text{ mm}$$

$$yy = \frac{-72}{\cos 3.64}$$

$$= -72.14 \text{ mm}$$

The new coordinate for the HJC location for Subject 1:

$$c = \begin{bmatrix} -55.51 \\ -72.14 \\ -25 \end{bmatrix} \text{ mm}$$

From these results it is clear that the coordinates found using ultrasound don't match the functional method prediction, however the z coordinate is fairly similar.

This procedure was then repeated for Subject 2, and the results below show the PD, Pelvic Angle (θ) and the final ultrasound prediction of the HJC in the correct local coordinate system.

$$PD = 223.5 \text{ mm}$$

$$\theta = 4.62^\circ$$

$$c = \begin{bmatrix} -65.21 \\ -55.18 \\ -7.5 \end{bmatrix} \text{ mm}$$

These results confirm that what was assumed to be the head of the femur seen on the ultrasound scan for Subject 2, is in fact not. The result calculated using this method was vastly different from that obtained using the functional method. It can therefore be concluded that it is not efficient to try and validate this functional method using ultrasound techniques since there are too many possible inaccuracies.

4.4. PREDICTIVE VALIDATION

Predictive methods for locating the HJC are still the main technique used in clinical settings. It is important then to compare the results obtained from the functional method to those of predictive regression equations. The regression equations used for this study are the ones proposed by Harrington *et al* in 2007. These equations were produced by comparing previous regression equations with functional methods validated by the use of MRI. These equations therefore, should be the most accurate to date.

The equations proposed by Harrington *et al* are shown below:

$$\hat{x} = -0.24PD - 9.9$$

$$\hat{y} = -0.30PW - 10.9$$

$$\hat{z} = 0.33PW + 7.3$$

Where PD represents the pelvic depth (distance between ASIS midpoint and PSIS midpoint) and PW is the Pelvic Width (distance between ASIS).

These variables can be calculated using the coordinates provided by the Nexus software. These were found for each of the new subjects, and four from Byrne's study last year. Subject 1's details are calculated below and the other 5 subjects' data is listed in the table to follow using the same procedure.

Subject 1

PD – Distance between the ASIS midpoint and PSIS midpoint. (This procedure is described in section 4.3.)

Therefore Subject 1 PD = 188.9mm

PW – Distance between Left and Right ASIS:

$$\begin{aligned}PW &= \sqrt{\Delta x^2 + \Delta y^2 + \Delta z^2} \\ &= \sqrt{244^2 + 9^2 + 16^2} \\ &= 245mm\end{aligned}$$

Substitute Values into Harrington's Equations:

$$\begin{aligned}\hat{x} &= -0.24PD - 9.9 \\ &= -0.24(188.9) - 9.9 \\ &= \underline{-55.236mm}\end{aligned}$$

$$\begin{aligned}\hat{y} &= -0.30PW - 10.9 \\ &= -0.30(245) - 10.9 \\ &= \underline{-84.4mm}\end{aligned}$$

$$\begin{aligned}\hat{z} &= 0.33PW + 7.3 \\ &= 0.33(245) + 7.3 \\ &= \underline{88.15mm}\end{aligned}$$

Predicted HJC (Relative to Midpoint of PW origin):

$$c = \begin{bmatrix} -55.24 \\ -84.40 \\ 88.15 \end{bmatrix} mm$$

This prediction must then be transformed into the same coordinate system used for the functional method, ie, the origin located at the right ASIS, this is done by

subtracting the distance in the z axis from half of the PW. Then sign convention must be considered.

Predicted HJC (Relative to right ASIS origin):

$$c = \begin{bmatrix} -55.24 \\ -84.15 \\ -34.35 \end{bmatrix} mm$$

The results for each subject are shown below.

Subject	PD (mm)	PW (mm)	Origin		Functional Prediction	
			PW Midpoint	Right ASIS	Orthogonal	Non- Orthogonal
1	188.9	245	$\begin{bmatrix} -55.24 \\ -84.40 \\ 88.15 \end{bmatrix}$	$\begin{bmatrix} -55.24 \\ -84.15 \\ -34.35 \end{bmatrix}$	$\begin{bmatrix} -36.10 \\ -123.20 \\ -27.43 \end{bmatrix}$	$\begin{bmatrix} -36.49 \\ -122.32 \\ -28.11 \end{bmatrix}$
2	223.5	244.5	$\begin{bmatrix} -63.54 \\ -84.25 \\ 87.99 \end{bmatrix}$	$\begin{bmatrix} -63.54 \\ -84.25 \\ -34.26 \end{bmatrix}$	$\begin{bmatrix} -90.83 \\ -93.58 \\ -31.47 \end{bmatrix}$	$\begin{bmatrix} -92.95 \\ -90.23 \\ -31.15 \end{bmatrix}$
3	206.8	235	$\begin{bmatrix} -59.53 \\ -81.4 \\ 84.85 \end{bmatrix}$	$\begin{bmatrix} -59.53 \\ -81.4 \\ -32.65 \end{bmatrix}$	Due to the lack of information provided by Paul Byrnes' previous work, His predicted HJC seemed highly inaccurate for the coordinate system he claimed to use, distances in the y axis range from -64mm (reasonable) to 9.8mm (Above ASIS – highly unlikely)	
4	218.5	263	$\begin{bmatrix} -62.34 \\ -89.8 \\ 94.09 \end{bmatrix}$	$\begin{bmatrix} -62.34 \\ -89.8 \\ -37.41 \end{bmatrix}$		
5	206.4	240	$\begin{bmatrix} -59.44 \\ -82.9 \\ 86.5 \end{bmatrix}$	$\begin{bmatrix} -59.44 \\ -82.9 \\ -33.5 \end{bmatrix}$		
6	264.5	276	$\begin{bmatrix} -73.38 \\ -93.7 \\ 98.38 \end{bmatrix}$	$\begin{bmatrix} -73.38 \\ -93.7 \\ -39.62 \end{bmatrix}$		

Table 4.1 - Summary of Regression and Functional Results

As can be seen in the above table the predictions using the regression equations produced by Harrington, are still not very similar to those provided by the functional method. For Subject 1, the x and z coordinates differ by 19 and 6.92mm respectively.

The biggest difference was experienced in the y coordinate of 39mm in the orthogonal axis. However it is a different story when comparing the predictions for Subject 2 where it was the x -axis that experienced the biggest difference of 27mm. From these results it can be seen that the ratio of STA is not always consistent for each individual, skin movement must also be taken into account for these inaccuracies. As can be seen between Subjects 1 and 2, the biggest differences occur in different axes, emphasizing that no matter what method is used to determine the HJC location there will still be random errors encountered due to the various techniques and individual body properties. These results share the same problem when comparing them to the non-orthogonal axis predictions, proving that each method, predictive or functional, still have underlying flaws that need to be addressed before an accurate prediction can be made.

4.5 MRI VALIDATION

The use of MR Imaging has been defined as the benchmark in locating the HJC, this is because it provides clear accurate images of inside the body allowing for easy visualization of internal structures. Due to the most definite results from the previous methods used, Subject 1 was chosen to undergo the MRI scan. The scanner used was a GE Medical Systems Signa 3.0T based at the Institution of Neuro Science, Southern General Hospital, Glasgow. Before scanning could commence the system was set with a field of view of 350mm to ensure a large enough area was scanned to incorporate both bony landmarks of the pelvis and the head of the femur. It was then set to take 126 slices at 2.5mm increments to achieve a good enough resolution for the overall images. In order to be able to determine the coordinate system for the

pelvis, cod liver oil capsules were taped onto the bony landmarks of the pelvis. The fatty liquid within these capsules would show clearly on the images where the bony landmarks were located. Once the data had been gathered it was then exported into a software program called Mimics 14.12 by Materialise. This software allows for the detection of the bony landmarks and corresponding distances. It also allows for a 3D image to be created using the 'slices' for better visualization but due to time constraints this was not possible. Instead the coordinates of the HJC were calculated using the same technique as used with the ultrasound but with far more accurate measurements. After scanning, nurses that were assisting with the MRI explained their own method for locating the hip joint centre. It involved manually locating the midpoint between the ASIS and a bony landmark at the pubis and moving roughly 1 inch medially. An image of this position on subject one is shown below.

However this method is only used to determine a rough area for the hip joint so the right area can be x-rayed therefore only producing a 2 dimensional coordinate on the frontal plane. This coordinate is (-30,-70)

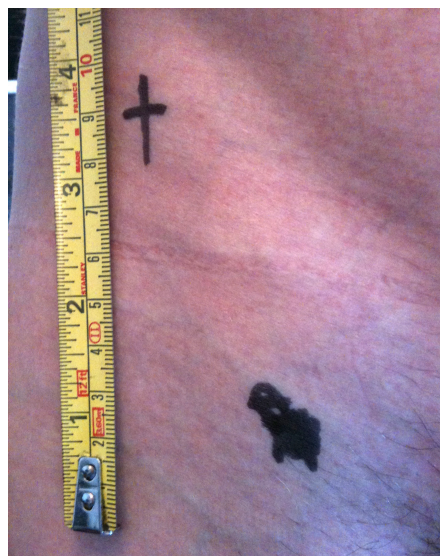


Figure 4.8 - Nurses Prediction

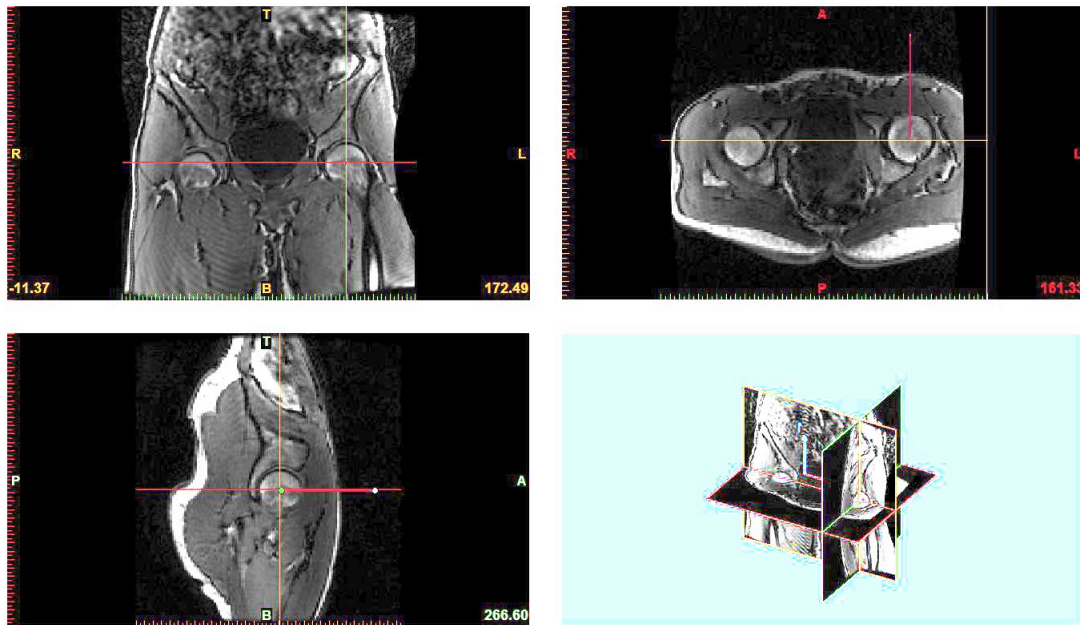


Figure 4.9 - Mimics Screenshots Displaying HJC

The images above are screenshots from the Mimics software showing that the HJC can be easily distinguished. From these, distances in the frontal plane were determined along with the angle of the pelvis in order to establish the location in the local axis system. Placing markers on the images, allows for anatomical positions to be seen in all ‘slices’, simplifying the task of positioning. The following images show the distances in the frontal plane in reference to the right ASIS.

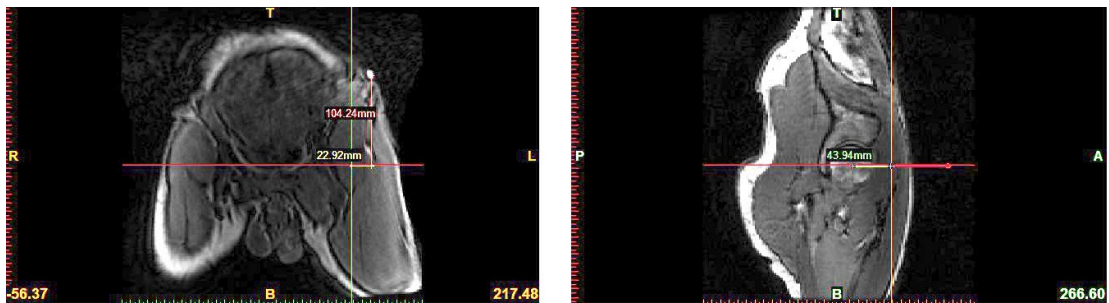


Figure 4.10 – Dimensioned MRI

As with the ultrasound, the angle of the pelvis must be taken into account in order to transform these coordinates from the frontal plane, to that of the local coordinate system. The angle of the pelvis is shown in the image below.



Figure 4.11 - Angle of Pelvis

Therefore using the same principles as the ultrasound method, the coordinates can then be transformed into the local coordinate system. However the distance in the x direction is taken from the centre of the cod liver oil tablet, where as the functional method used the distance from the centre of the reflective markers. The radii of both tablet and marker are different so this needs to be compensated for in the MRI results. This however only affects the x-axis coordinate. A difference of approximately 5 mm was found between the two.

Non-transformed HJC:

$$c = \begin{bmatrix} -38.94 \\ -104.24 \\ -22.92 \end{bmatrix} mm$$

Transformed HJC:

$$c = \begin{bmatrix} -39.47 \\ -105.52 \\ -22.92 \end{bmatrix} mm$$

MRI is proven to be one of the best forms of imaging used in the medical industry, consequently this result will be taken to be the true location of the HJC for Subject 1 in this study.

4.6 RESULT COMPARISON

The table below shows a comparison of all valid results taken for Subject 1.

Functional Method		Harrington RE	Ultrasound	MRI
Orthogonal	Non-Ortho			
$\begin{bmatrix} -36.10 \\ -123.20 \\ -27.43 \end{bmatrix}$	$\begin{bmatrix} -36.49 \\ -122.32 \\ -28.11 \end{bmatrix}$	$\begin{bmatrix} -55.24 \\ -84.15 \\ -34.35 \end{bmatrix}$	$\begin{bmatrix} -55.51 \\ -72.14 \\ -25.00 \end{bmatrix}$	$\begin{bmatrix} -39.47 \\ -105.52 \\ -22.92 \end{bmatrix}$

Table 4.2 - Result Comparison

From these results it can be seen that no method of HJC prediction compares well with that produced from the MRI. This is due to the Soft Tissue Artifact which least affect the z coordinate for Subject 1. However, the biggest errors are seen in Harrington's regression equations, exhibiting the largest amount of error in each of the 3 coordinates. The functional method performs the best but is still subject to a vast amount of error in the y direction. The two dimensional prediction was also significantly off that of the MRI, being similar to those produced from the ultrasound. However this is not used as a precise indicator of the HJC location and just a rough area.

4.7 DISCUSSION SUMMARY

This study set out to attempt to validate some of the methods already in existence used to determine the location of the HJC. Using the MRI as the true coordinate, the results proved to be far from accurate for each method. The functional method proved to work well on the mechanical model test, however when it came to subject testing it was far from accurate. The only similarity was in the x -axis with a difference of only 3mm. One of the main factors contributing to these errors is the

presence Soft Tissue Artifact. For Subject 1 it was seen that this was most evident in the y coordinate, producing errors up to 33.38mm from the ultrasound test. However these results differ from Subject 2 whom, even though not subject to MRI validation, experienced the maximum displacements in the x direction. This proves that Soft Tissue Artifact differs from individual to individual.

Soft Tissue Artifact does not only affect the thigh markers. If the markers are not placed accurately on the bony landmarks of the pelvis, this will produce an inaccurate coordinate system thus producing invalid results. Bony landmarks are not actual points but are ridges under the skin and may be hard to find on some individuals because there may be a concealing layer of tissue. It is difficult to keep the same level of consistency in marker position, which depend entirely on the perceived location of the bony landmarks and could differ from their actual position. These errors in initial positioning could be several mm, reducing the accuracy of the local coordinate system.

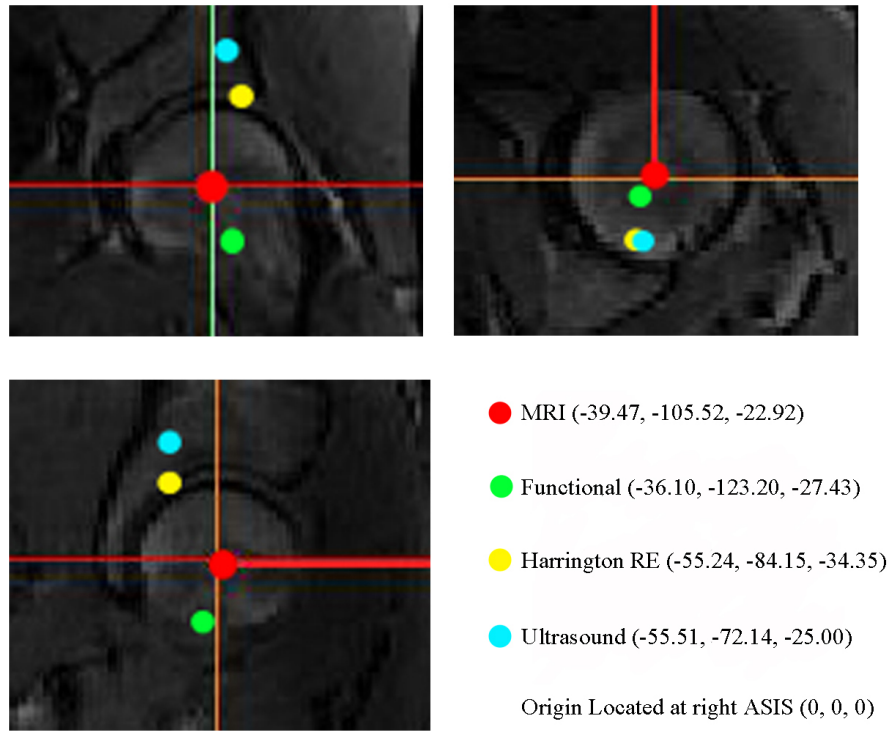


Figure 4.12 - Location Summary (coordinates in mm)

Above is a summary of the HJC positions and coordinates found for subject one imposed onto the MRI images obtained during the study, the origin is located at the right ASIS, conforming to the system produced by WU (2002) described in section 2.2.

CHAPTER 5. CONCLUSION

The accurate location of the HJC is critical in determining joint kinematics during gait analysis. The developments of functional methods have improved predictions greatly but are still far from accurate. Findings show errors as little as 3mm in the x-axis and as large as 18mm in the y-axis show that the results cannot be relied upon. The validation techniques that have been used in the past to not only to validate findings but also to produce their own regression equations, themselves are subject to inaccuracy, thus rendering their own methods void. Ultrasound is particularly difficult without the use of high-powered specialized equipment to determine an accurate coordinate, producing the greatest errors of up to 33mm. The most disturbing conclusion that can be taken from this study, is that the regression equations that are still favoured in clinical settings and are considered to be good enough, proved to be the least accurate.

CHAPTER 6. FUTURE WORK

This research shows that the issue of Soft Tissue Analysis is still a serious problem when trying to determine the location of the Hip Joint Centre. The subject requires a lot more investigation. Although the developments of the functional methods have decreased the errors, they are still a long way off the true coordinate provided by the MRI validation. To try and resolve this matter, further investigation should be carried out regarding the relationship between Soft Tissue Artifact and the HJC coordinate. Using MRI as validation, it should be possible to combine both functional and predictive methods to produce a set of regression equations. The values entered into these equations should be read from a table combining the patients BMI and body fat percentage. This would produce more accurate equations that are more personalized to a particular individual, hopefully providing more accurate results. This would be beneficial in clinical settings where the uses of functional methods are practiced.

Alternatively, this proposed enhanced information could be used to develop further equations dealing with the compensation of Soft Tissue Artifact and combined with functional methods with the aim of reducing the errors of these methods further. However due to the expense of systems that are required to apply functional methods, it is more likely, for the time being, to remain as a tool for the further development in regression equations.

REFERENCES

- P.A. Byrne, 2010, Prediction of the Hip Joint Centre from Externally Placed Markers in Gait Analysis Studies, MSc Thesis, University of Strathclyde, Glasgow.
- V Camomilla, A Cereatti, G Vannozzi, A Cappozzo (2006); “An optimization protocol for hip joint centre determination using the functional method”; *Journal of Biomechanics* **39** p1096-1106
- A.C. Campbell, D.G. Lloyd, J.A. Alderson, B.C. Elliott (2009); “MRI development and validation of two new predictive methods of glenohumeral joint centre location identification and comparison with established techniques”; *Journal of Biomechanics* **42** p1527-1537
- A Cereatti, V Camomilla, A Cappozzo (2004); “Estimation of the centre of rotation: a methodological contribution”; *Journal of Biomechanics* **37** p413-416
- A Cereatti, M Donati, V Camomilla, F Margheritini, A Cappozzo (2009); “Hip joint centre location: An ex vivo study”; *Journal of Biomechanics* **42** p818-823
- A Cereatti, F Margheritini, M Donati, A Cappozzo (2010); “Is the human acetabulofemoral joint spherical?”; *The Journal of Bone & Joint Surgery (Br)* **Vol.92(2)** p311-314
- R.B Davis III, S Öunpuu, D Tyburski, J.R Gage (1991); “A gait analysis data collection and reduction technique” *Human Movement Science* **10** p575-587
- R M Ehrig (2006); “A survey of formal methods for determining the centre of rotation of ball joints”; *Journal of Biomechanics* **39** p2798-2809
- S.S.H. Gamage & Lasenby (2002); “New least squares solutions for estimating the average centre of rotation and axis of rotation”; *Journal of Biomechanics* **35** p87-93
- K. Halvorsen (2003); “Bias compensated least squares estimate of the centre of rotation”; *Journal of Biomechanics* **36** p999-1008
- K Halvorsen, M Lesser, A Lundberg (1999); “A new method for estimating the axis of rotation and the centre of rotation”; *Journal of Biomechanics* **32** p1221-1227
- L Harding, M Barbe, K Shepard, A Marks, R Ajai, J Lardiere, H Sweringa (2003); “Posterior-Anterior Glide of the Femoral Head in the Acetabulum: A

Cadaver Study”; *Journal of Orthopaedic and Sports Physical Therapy* **33** p118-125

- M.E. Harrington (2007); “Prediction of the hip joint centre in adults, children and patients with cerebral palsy based on magnetic resonance imaging”; *Journal of Biomechanics* **40** p595-602
- M.O. Heller, C. König, H. Graichen, S.Hinterwimmer, R.M.Ehrig, G.N. Duda, W.R. Taylor (2007); “A new model to predict in vivo human knee kinematics under physiological-like muscle activation” *Journal of Biomechanics* **40** pS45-S53
- J.L. Hicks, James G. Richards (2005); “Clinical applicability of using spherical fitting to find hip joint centres” *Gait & Posture* **22** p138-145
- A Leardini, A Cappozzo, F Catani, S Toksvig-Larsen, A Petitto, V Sforza, G Cassanelli, S Giannini (1999); “Validation of a functional method for estimation of hip joint centre location” *Journal of Biomechanics* **32** p99-103
- G Lenaerts, W Bartels, F Gelaude, M Mulier, A Spaepen, G Van der Perre, I Jonkers (2009); “Subject-specific hip geometry and hip joint centre location affects calculated contact forces at the hip during gait” *Journal of Biomechanics* **42** p1246-1251
- F.H. Martini; “The Hip Joint” *Fundamentals of Anatomy & Physiology* (2009-8th Edition) **9** p283
- M H Schwartz (2009); “A new method for estimating joint parameters from motion data”; *Journal of Biomechanics* **38** p107-116
- R Stagni, A Leardini, A Cappozzo, MG Benedetti, A Cappello (2000); “Effects of hip joint centre mislocation on gait analysis results” *Journal of Biomechanics* **33** p1479-1487
- H J Woltring (1990); “Data processing and error estimation”; In: N. Berme, A. Capozzo (Eds.), *Biomechanics of Human Movement*, p203-237
- Ge Wu (2002); “ISB recommendation on definitions of joint coordinate system of various joints for reporting of human joint motion – part I: ankle, hip, spine” *Journal of Biomechanics* **35** p543-548

Online Material

- How Gait Analysis Has Emerged as Tool for Biometric Identification? [Online], available at; <http://techbiometric.com/articles/how-gait-analysis-has-emerged-as-tool-for-biometric-identification/>, [Accessed; 14/7/2011]

- MRI Scan [Online], available at; <http://www.patient.co.uk/health/MRI-Scan.htm>, [Accessed: 31/7/2011]
- X-rays [Online], available at; http://www.netdoctor.co.uk/health_advice/examinations/x-ray.htm, [Accessed;30/7/2011]
- X-Rays [Online], available at; <http://science.hq.nasa.gov/kids/imagers/ems/xrays.html>, [Accessed;30/7/2011]
- The Yorkshire Foot Surgery & Biomechanics Clinic [Online], available at; <http://www.chiropodyonline.co.uk/gan.htm>, [Accessed; 18/7/2011]

APENDIX I – MATLAB Final Script and Functions

Final Script

```
%% clean the workspace
hold off
clear all
close all

flag = 2;

if flag == 1

    %% load the data:
    % the matrix P of all points and indices of the tracks

    %Craig's mechanical part
    dynamic3

    %% extract tracks
    % thigh tracks
    T(:, :, 1)=P(:, T1ind);
    T(:, :, 2)=P(:, T2ind);
    T(:, :, 3)=P(:, T3ind);
    T(:, :, 4)=P(:, T4ind);
    % hip tracks
    H(:, :, 1)=P(:, H1ind);
    H(:, :, 2)=P(:, H2ind);
    H(:, :, 3)=P(:, H3ind);

    % centre in absolute coordinates
    CE = H(:, :, 1);

    %% coordinate transformation
    % compute the coordinate vectors using the hip tracks
    [s1 s2 s3] = coordinate_vectors (H(:, :, 1), H(:, :, 2), H(:, :, 3));

elseif flag == 2

    %Craig's object data
    points_Me103

    %% extract tracks
    % thigh tracks
    T(:, :, 1)=P(:, T1ind);
    T(:, :, 2)=P(:, T2ind);
    T(:, :, 3)=P(:, T3ind);
    T(:, :, 4)=P(:, T4ind);
    % hip tracks
    F1=P(:, F1ind);
    F2=P(:, F2ind);
    R1=P(:, R1ind);
```



```

R2=P(:,R2ind);

% centre in absolute coordinates
CE=F1;

%% coordinate transformation
% compute the coordinate vectors using the hip tracks
[s1 s2 s3] = coordinate_vectors_hip (F1,F2,R1,R2);
[s1 s2 s3] = coordinate_vectors (F1,F2,R1);

end

% transform the thigh tracks into the relative coordinate system
for i=1:4
    Pr(:,3*i-2:3*i) = relative_coordinates (T(:, :, i),CE,s1,s2,s3);
end

% find the centre of rotation and radii
[c r A b] = GamageLasenby(Pr);
c
r

%% generate the spheres
% points of the unit sphere
[X,Y,Z] = sphere(20);
% expand to the radius r and shift to the centre c
for i=1:4
    XX(:, :, i) = X*r(i) + c(1);
    YY(:, :, i) = Y*r(i) + c(2);
    ZZ(:, :, i) = Z*r(i) + c(3);
end

%% plot some of the original thigh tracks
figure(1)
for i=1:2
    plot3(T(:,1,i),T(:,2,i),T(:,3,i),'.')
    hold on
    axis equal
end
axis tight

%% plot all thigh data in relative coordinates
figure(2)
hold on
for i=1:4
    plot3(Pr(:,3*i-2),Pr(:,3*i-1),Pr(:,3*i),'.')
end
axis equal
axis tight

%% plot each thigh track with the sphere
for i=1:4
    figure
    plot3(Pr(:,3*i-2),Pr(:,3*i-1),Pr(:,3*i),'.')
    hold on

```

```

        mesh(XX(:,:,i),YY(:,:,i),ZZ(:,:,i))
        axis equal
        axis tight
    end

%% Assessment
disp(['condition number of A: ',num2str(cond(A))])
disp(' ')
disp('Accuracy of the sphere fit for each track and distances to the
centre')
disp('          rms error    bias    ave_dist    min_dist
max_dist')
n=size(Pr,1); % number of points
for i=1:4
    diffs = Pr(:,3*i-2:3*i) - ones(n,1)*c';
    dists = sqrt(sum(diffs.*diffs,2)); %distances to the computed
centre
    ave_dist = sum(dists)/length(dists);
    max_dist = max(dists);
    min_dist = min(dists);
    rad_rms = sqrt(sum((dists - r(i)).^2)/n);
    rad_bias = sum(dists)/n - r(i);
    disp([int2str(i), '-th track: ', num2str(rad_rms, '%.4f'), '
', num2str(rad_bias, '%.2e'), ...
        ' ', num2str(ave_dist, '%.4f'), '
', num2str(min_dist, '%.4f'), ' ', num2str(max_dist, '%.4f')])
end

if flag == 1

    %% plot all hip tracks and the track of the computed centre
    figure
    hold on
    for i=1:3
        plot3(H(:,1,i),H(:,2,i),H(:,3,i), '.'))
    end
    cabs = absolute_coordinates (ones(n,1)*c',CE,s1,s2,s3);
    plot3(cabs(:,1),cabs(:,2),cabs(:,3), 'r')
    axis equal
    axis tight

end

% %% plot the hip data in relative coordinates (needed for debugging
only)
% each track must collapse into one point
% figure(356)
% for i=5:7
% Pr(:,3*i-2:3*i) = relative_coordinates (P(:,3*i-
2:3*i),H(:, :,1),s1,s2,s3);
% plot3(Pr(:,3*i-2),Pr(:,3*i-1),Pr(:,3*i), '.r')
% hold on
% end
% axis equal
% axis tight

```

absolute_coordinates

```
function pnew = absolute_coordinates (p,c,s1,s2,s3)
% given n points in relative coordinates and the relative coordinate
% system for each,
% compute the absolute coordinates of all points
% p -- an (n x 3)-matrix whose rows are relative coordinates to be
% transformed
% c -- an (n x 3)-matrix whose rows are absolute coordinates of
% the origins of the
% relative coordinate systems
% s1,s2,s3 -- (n x 3)-matrices of unit vectors of the relative
% coordinate systems
% pnew -- the (n x 3)-matrix of absolute coordinates

% for each moment, the transformation matrix is the transpose of the
% matrix given by s1,s2,s3,
% and the coordinates of the absolute unit vectors are the columns
% of this matrix:
t1 = [s1(:,1) s2(:,1) s3(:,1)];
t2 = [s1(:,2) s2(:,2) s3(:,2)];
t3 = [s1(:,3) s2(:,3) s3(:,3)];

% find the relative coordinates of the origin of the absolute system
cnew = -[sum(c.*s1,2) sum(c.*s2,2) sum(c.*s3,2)];

% the coordinates are the inner products of p-cnew with t1,t2,t3
p=p-cnew;
pnew = [sum(p.*t1,2) sum(p.*t2,2) sum(p.*t3,2)];
```

coordinate_vectors_hip

```
function [s1 s2 s3] = coordinate_vectors_hip (f1,f2,r1,r2)
% computes three arrays of unit coordinate vectors from three arrays
of 3D points
% f1,f2,r1,r2 - (n x 3)-matrices containing for each n the
coordinates of the two front (f1,f2)
%           and two rear (r1,r2) markers on the hip
% s1,s2,s3 - (n x 3)-matrices containing for each n the coordinates
of three unit vectors that
%           build an orthogonal coordinate system generated by
orthogonalising p2-p1 and p3-p1,
%           and adding their cross product
% The origins of the new coordinate systems will be at f1
% Assumes that the points in the rows of p1,p2,p3 are not collinear
%
% Oleg Davydov 25/07/2010

%% compute the third coordinate directions (z-axis) as difference of
f2 and f1
z=f2-f1;
z=normalise(z); %normalisation

%% compute the first coordinate directions (x-axis)
x=(r1+r2-f1-f2)/2;

% orthogonalise x to z
pr = sum(x.*z,2); % compute projections on z
x=x-z.*pr(:,[1 1 1]);% orthogonalisation of x

%normilise x
x=normalise(x);

%% compute the second coordinate directions (y-axis) using the cross
product
y = cross(z,x,2);
y=normalise(y);

s1=x;
s2=y;
s3=z;

function v = normalise(v)
% normalise each row of an (n x 3)-matrix

norms = sqrt(sum(v.*v,2));
v=v./norms(:,[1 1 1]);
%v=v./norms(:,ones(3, 1));
```

relative_coordinates

```
function pnw = relative_coordinates (p,c,s1,s2,s3)
% given n points in absolute coordinates and the relative coordinate
% system for each,
% compute the relative coordinates of all points
% p -- an (n x 3)-matrix whose rows are absolute coordinates to be
% transformed
% c -- an (n x 3)-matrix whose rows are absolute coordinates of
% the origins of the
% relative coordinate systems
% s1,s2,s3 -- (n x 3)-matrices of unit vectors of the relative
% coordinate systems
% pnw -- the (n x 3)-matrix of relative coordinates
%
% Oleg Davydov 02/06/2010
```

```
% the coordinates are the inner products of p-c with s1,s2,s3
p=p-c;
pnw = [sum(p.*s1,2) sum(p.*s2,2) sum(p.*s3,2)] ;
```

GamageLasenby

```
function [c r A b] = GamageLasenby(P)
% Computing the centre of rotation from a number of tracks on
% concentric spheres
%
% Reads a matrix P of size n x 3p, where p is the number of tracks
% and n the number of points in each track.
% In each track, the three consecutive columns correspond to x-, y-
% and z-coordinates.
%
% Returns:
% c -- the coordinates of the centre of rotation
% r -- the p-vector of radii of the spheres of the tracks
% A,b -- the matrix and RHS of the linear system to investigate
% numerical stability
%
% Oleg Davydov 04/06/2010

% number of points in the tracks
n = size(P,1);

% number of tracks
p = size(P,2)/3;

%% various averages and outer products for all tracks
av = reshape(mean(P),3,[]);
PP = P.*P; % squares of all entries of P
%av2 = sum(reshape(sum(PP),3,[]))/n;
av2 = zeros(1,p);
av3 = zeros(3,p);
Avop = zeros(3,3*p); %outer products of averages
Pt=P';
Pop=zeros(3*n,3*p); % outer products of the points in 3x3-blocks
for i=1:p
```

```

    indx = 3*i-2:3*i;
    sqn=sum(PP(:,indx),2);% squared norms of all points of the p-th
track
    av2(i) = sum(sqn)/n;
    av3(:,i) = sum(P(:,indx).*sqn(:,[1 1 1]))'/n;
    tav = av(:,i);
    Avop(:,indx)=tav*tav';
    Pop(:,indx(1))=reshape(Pt(indx,:),3*n,1);
    Pop(:,indx(2))=reshape(Pt(indx,:),3*n,1);
    Pop(:,indx(3))=reshape(Pt(indx,:),3*n,1);
end
Pop=Pop.*P(reshape([1:n; 1:n; 1:n],3*n,1),:); % contains the outer
products in 3x3-blocks

%% setting up the linear system
% RHS
b = sum(av3 - av.*av2([1; 1; 1],:),2);
% sum up the outer product matrices in columns, average and subtract
the matrix avop
Sop=[sum(Pop(1:3:3*n-2,:)); sum(Pop(2:3:3*n-1,:));
sum(Pop(3:3:3*n,:))]/n - Avop;
% sum up in rows to obtain the matrix of the linear system
A=2*[sum(Sop(:,1:3:3*p-2),2) sum(Sop(:,2:3:3*p-1),2)
sum(Sop(:,3:3:3*p),2)];

% solve the linear system to obtain the centre or rotation
c=A\b;

% find the radii
P=P-c(ones(n,1)*reshape([ones(1,p); 2*ones(1,p);
3*ones(1,p)],1,3*p));
P = P.*P;
r = sqrt(sum(reshape(sum(P),3,p))/n);

```